OPTIMAL SPHERICAL GEODESIC CURVATURE CONSTRAINED PATHS

A Thesis

by

ATHINDRA PAVAN

Submitted to the Graduate and Professional School of
Texas A&M University
in partial fulfillment of the requirements for the degree of

MASTER OF SCIENCE

Chair of Committee,	Swaroop Darbha
Committee Members,	Kumbakonam Rajagopal
	John Valasek
Head of Department,	Guillermo Aguillar

August 2021

Major Subject: Mechanical Engineering

ABSTRACT

Path planning for vehicles is an essential study that must be undertaken to make good use of resources such as fuel (which is always a limited resource) to ascertain that a vehicle/robot completes its mission efficiently. The current study deals with the path planning of a Dubins' vehicle on a sphere. A Dubins' vehicle is one that moves only forwards, with a constant speed and with a minimum turning radius constraint; and is named after L.E. Dubins due to his seminal work [1] on the nature of optimal curves in the plane. The result being that optimal paths must be of the following types only: CSC, CCC, SC, CS, CC, or C can be optimal. This study aims to understand the nature of optimality of the Dubins' type paths on a sphere.

The main tools employed are Pontryagin's Minimum Principle and the Sabban frame (same setup as in Monroy-Pérez's work [2]). The final result obtained as a result of analytical study and corroboration with numerical computation is that Dubins' type paths are optimal on the sphere for $r \in \left(0, \frac{1}{2}\right]$ on account of the $CCCC$ type path being non-optimal in the same interval.

ACKNOWLEDGEMENTS

I would like to thank my family for supporting me in all ways imaginable and making it possible for me to do my graduate studies at Texas A&M University.

I am forever indebted to all the teachers and professors I have had over the course of my life for moulding me into the person I am today and making me capable of completing this Masters' program.

This terrific journey would be unimaginable without my fellow mechanical engineering graduate students, who were always there to support me in my studies and learning.

I count myself extremely lucky to have had the best support system of friends consisting of the BP, Aashriii, Seems, Kebs, Melvin, Julian, Aarsh, Shubhendra, Allen, Nun, C, Gar, and Swaps.

CONTRIBUTORS AND FUNDING SOURCES

Contributors

This work was supported by a thesis committee consisting of Dr. Swaroop Darbha and Dr. Kumbakonam Rajagopal of the Department of Mechanical Engineering and Dr. John Valasek of the Department of Aerospace Engineering.

The interactions with Dr. Manyam Satyanarayana and Dr. David Casbeer from Air Force Research Lab (AFRL) have been invaluable in understanding the problem better.

All other work conducted for the thesis was completed by the student independently.

Funding Sources

Graduate study was supported by a fellowship from the Department of Mechanical Engineering at Texas A&M University. No other outside source of funding was provided.

TABLE OF CONTENTS

Page

LIST OF FIGURES

FIGURE Page

1. INTRODUCTION AND LITERATURE REVIEW

It is the current work's objective to characterize optimal paths traversed by Dubins' vehicles on a sphere. In the field of path planning, there are two main types of vehicles that are considered in study. These are: the Dubins' vehicle and the Reeds-Shepp vehicle. The vehicle is treated as a point mass and the kinematics of the vehicle is studied. A Dubins' vehicle is one that is defined to be able to move only forwards, while a Reeds-Shepp vehicle is one that can move both forwards and backwards. The Reeds-Shepp vehicle is studied in [3]. A Dubins' path is one that is traversed by a Dubins' vehicle. This name for this type of problem is due to the work of L.E. Dubins [1]. A Dubins' vehicle is one that has a minimum turning radius constraint, moves only forwards, and has a constant speed. This means that the vehicle is not allowed to make sharp turns and the tightest turn it can make is a circular arc of the minimum turning radius specified. These arcs are called tight circular arcs or small circular arcs in the rest of the document.

On the plane, a Dubins' vehicle can only make tight turns or travel in a straight line in order for the path to be optimal. Moreover, they can only be of certain types. C is used to represent a tight circle arc and S is used to represent a straight line path. Thus, an optimal path can only have S and C segments. This crucial result is studied in [1] using only geometrical arguments and in [4] using Pontryagin's minimum principle. The main tool used in this work is the Pontryagin's principle as well. The types of paths traversed by a Dubins' vehicle that can be optimal on the plane are called the Dubins' type paths and are the following: CSC, CCC, CS, SC, S, C. Essentially, optimal curves on the plane can only contain S or C segments and curves containing 4 or more concatenations are non-optimal.

In the current work, since curves on the sphere are being studied, the Sabban frame is used. Sabban frames are a sub-category of Frenet-Serret frames which are studied extensively in most classical differential geometry texts like [5]. The Sabban frame and Pontryagin's minimum principle are the main tools used. This is the same as the setup used in [2]. Note that C is used to represent a tight circle arc on the sphere (same as in the case of the plane), and G is used to rep-

resent a great circle arc on the sphere (which is equivalent to the straight line on the plane). This makes sense since the geodesic on a plane is the straight line and that on the sphere is the great circle. In [2], it has shown that Dubins' type paths are optimal for when minimum turning radius constraint $r = \frac{1}{\sqrt{2}}$ and the radius of the sphere $R = 1$. Using the same concepts discussed in [1], stating that if $CCCC$ paths are shown to be non-optimal, then Dubins' type paths have to be non-optimal, one may show that Dubins' type paths are optimal on the sphere as well.

Other methods of proof for the same results obtained in [1] have been constructed. An example of such work is [6]. A lot of work has been and is being done in the field of path planning that additionally deals with multiple way points and even multiple vehicles being considered at the same time. This sort of problem might require algorithms from the field of operations research (like the Bellman-Ford algorithm, A^* algorithm, etc) combined with the concept of Dubins'/Reeds-Shepp type path planning. Examples of the kind of work being done involving multiple way points in the path of a vehicle are [7] and [8]. Though the current work is analytical in nature and uses numerical computation for just corroboration of proved results, there are other bodies of work which deal with determining algorithms for finding the shortest distance paths using concepts from graph theory and numerical analysis. An example of such work is [9].

Pontryagin's Minimum Principle (sometimes referred to as Maximum Principle as well) is the main technique used in this work. It is a central result that is used in the field of optimal controls and has tremendous applications in the field of differential geometry as well. Insights into how optimal control theory and differential geometry are related can be gained from reading [10] which is a historical perspective on the development of the field of optimal controls.

In the current work, the equivalent of all the basic proofs for Dubins' paths on the plane are worked out for Dubins' paths on the sphere. Then, the main result is arrived at, which shows that when r (the minimum turning radius) is in the interval $\left(0, \frac{1}{2}\right]$ and R (the radius of the sphere) equals 1, the Dubins' type paths must be optimal, i.e., when $r \in \left(0, \frac{1}{2}\right]$ and $R = 1$, optimal paths can only be of the following types: CGC, CCC, CG, GC, G, C.

2. MATHEMATICAL FORMULATION

2.1 Frames for studying spherical curves

Let s denote arc length, and $X(s)$ be a C^1-smooth spherical curve. Let $T(s) := \frac{dX}{ds}$ (denoted by $X'(s)$). Then, $T(s)$ is a unit vector as $ds^2 =< dX, dX >$. Define the cross product $N(s) = X(s) \wedge T(s)$. Defining $u(s) :=< T'(s), N(s) >$. Then,

$$T'(s) =< T'(s), X(s) > X(s) + < T'(s), N(s) > N(s) = -X(s) + u(s)N(s).$$

Similarly,

$$N'(s) = \underbrace{X'(s) \wedge T(s)}_{=0} + X(s) \wedge T'(s) = -u(s)T(s).$$

Putting everythnig together,

$$\begin{aligned} X'(s) &= T(s), \\ T'(s) &= -X(s) + u(s)N(s), \\ N'(s) &= -u(s)T(s). \end{aligned}$$

The term $u(s)$ is the geodesic curvature of the spherical curve. If $u(s) = 0$, it implies that $< T'(s), X(s) \wedge T(s) >= 0$, i.e., $T'(s)$ is perpendicular to the plane containing $X(s)$ and $T(s)$, i.e., the component of $T'(s)$ perpendicular to the plane containing the great circle is 0. If $u(s) \neq 0$, the curve has a tendency to move out of plane of $X(s)$ and $T(s)$ and it is a measure of how out-of-plane it will be.

2.2 Shortest path problem formulation

Consider the problem of determining the path of shortest length of a path to be taken by a rigid body connecting specified initial and final configurations. The variable s denotes the distance travelled along the path. The configuration of the rigid body is given by the three vectors $X(s), T(s)$

and $N(s)$; the vector $X(s)$ denotes the current location of the (center of mass of the) rigid body, $T(s)$ denotes the longitudinal direction, i.e., tangent to the path at $X(s)$ and $N(s) = X(s) \times T(s)$. By stacking $X(s), T(s), N(s)$, can specify a matrix $R(s) \in SO(3)$; $R(s)$ completely specifies the configuration of the rigid body on the unit sphere.

Suppose the initial configuration of the sphere is I_3, the 3×3 identity matrix; suppose the final configuration is given by $R_f \in SO(3)$. The problem of determining the path of shortest length connecting the two configurations can be expressed as the following variational problem:

$$J \;=\; \min \int_0^L 1 \, ds \tag{2.1}$$

subject to

$$\frac{dX}{ds} = T(s), \qquad \frac{dT}{ds} = -X(s) + u(s)N(s), \qquad \frac{dN}{ds} = -u(s)T(s), \tag{2.2}$$

subject to the boundary conditions

$$R(0) = I_3, \qquad R(L) = R_f. \tag{2.3}$$

The term $u(s)$ (or simply, u) is the scalar control input and represents the geodesic curvature; it is a measure of how the path is differing from the geodesic (great circle here). We assume that $u(s)$ is bounded by U_{max}, i.e., $|u(s)| \leq U_{max}$.

Let $r = \frac{1}{\sqrt{1+U_{max}^2}}$; let C denote a circular arc of radius r and G denote a greater circular arc (of radius 1). We denote concatenation of arcs in the order specified by the sequence of letters; for example, a path of type CGC involves concatenation of three arcs - the first arc is a smaller circular arc of radius r, the second one is a great circular arc and the third one is a smaller circular arc. Please note that the end points of the circular arc segment must be compatible at the points of concatenation, with the configuration of the body at the end of the previous circular arc being identical to the configuration at the beginning of the following circular arc. For example, in a CGC

path, the configuration of the body at the end of the first smaller circular arc must be identical to the configuration at the beginning of the greater circular arc; similarly, the configuration of the body at the end of the greater circular arc must be identical to the configuration at the beginning of the second circular arc.

3. MAIN RESULTS

The main result of this work is as follows:

Theorem 3.0.1. *If $0 < r \leq \frac{1}{2}$, the optimal path consists can only be of one of the six types: CGC, CCC, CG, GC, CC, G, or C.*

This is a generalization of characterization of optimal Dubins paths for planar systems to Dubins paths on a sphere.

The main tool used is Pontryagin's minimum principle and the main result is proved using the following intermediate results:

- Using Pontryagin's minimum principle, we show that the control actions are piecewise constant and the constant can be one of the three values, i.e., $u(s) \in \{U_{max}, 0, -U_{max}\}$. This is given in Lemmas 2.2 and 2.3.

- Each of the piecewise constant control actions results in a smaller circular arc (C) of radius r if $u(s) \neq 0$ or a great circular arc of radius 1. This is shown in Lemma 2.4. Together with Lemmas 2.2 and 2.3, this result implies that the optimal path is a concatenation of smaller circular arcs and great circular arcs.

- Non-optimality of a non-trivial concatenation of four circular arcs rules out the possibility of four or more circular arcs in the optimal path.

- If two great circular arcs are concatenated in succession, compatability at the point of concatenation implies that it cannot be a point of inflexion and hence, degenerates to a single great circular arc. Non-triviality imposes that two great circular arcs therefore be non-contiguous in the concatenation. This restricts the possible concatenations with four circular arcs for further investigation to one of the following eight possibilities – (1) CCCC, (2) CCCG, (3) CCGC, (4) CGCC, (5) GCCC, (6) CGCG, (7) GCCG, (8) GCGC. Non-optimality of paths of type GCG, GCC or CCG rules out the optimality of all paths but the CCCC path;

moreover, non-optimality of a CCG path implies the non-optimality of GCC path by symmetry. Hence, in Lemma 2.6, we show the non-optimality of GCG and GCC paths and use Lemma 2.5 for preparing the necessary background material for this lemma.

- Finally, we focus on showing that a CCCC path is not optimal if $0 < r \leq \frac{1}{2}$; the restriction on r appears only in this section of the theorem in the proof presented in this work.

4. PROOF

To apply Pontryagin's minimum principle, define the Hamiltonian through the dual/adjoint variables $\lambda_1(s), \lambda_2(s), \lambda_3(s)$ as:

$$\begin{aligned} H(s;\lambda_1,\lambda_2,\lambda_3) &= 1+<\lambda_1, T>+<\lambda_2, -X+uN>+<\lambda_3, -uT> \\ &= 1+<\lambda_1, T>-<\lambda_2, X>+u\{<\lambda_2, N>-<\lambda_3, T>\}. \end{aligned}$$

Define:

$$A := <\lambda_2, N>-<\lambda_3, T>, \tag{4.1}$$

$$B := <\lambda_3, X>-<\lambda_1, N>, \tag{4.2}$$

$$C := <\lambda_1, T>-<\lambda_2, X>. \tag{4.3}$$

It is easy to verify that

$$\frac{dA}{ds} = B, \qquad \frac{dB}{ds} = -A+uC, \qquad \frac{dC}{ds} = -uB. \tag{4.4}$$

and

$$H = 1 + C + uA. \tag{4.5}$$

through the following sequence of lemmas:

Lemma 4.0.1. *(i) Optimal control action is given by*

$$u = \begin{cases} -U_{max}, & A > 0, \\ U_{max}, & A < 0, \end{cases} \tag{4.6}$$

(ii)

$$A(s) \equiv 0, \quad \forall s \in [a,b) \implies u(s) \equiv 0, \quad \forall s \in [a,b).$$

Proof. (i) From Pontryagin's minimum principle, u minimizes H pointwise; hence,

$$u(s) = \begin{cases} -U_{max}, & A(s) > 0, \\ U_{max}, & A(s) < 0, \end{cases} \tag{4.7}$$

and is undetermined if $A = 0$.

(ii)

$$A(s) \equiv 0 \implies \frac{dA}{ds} \equiv 0 \implies B(s) \equiv 0 \implies \frac{dC}{ds} \equiv 0.$$

This implies that $C(s) = C_0$, but by Pontryagin's Minimum Principle, $H \equiv 0 \implies C_0 = -1$. Since $B(s) \equiv 0$, we have

$$\frac{dB}{ds} = 0 \implies -A(s) + u(s)C(s) = 0 \implies u(s)C_0 \equiv 0 \implies u(s) \equiv 0.$$

■

Note that $u(s) \equiv 0$ if and only if $A(s) \equiv 0$; otherwise, $u(s)$ will take a value of either $-U_{max}$ or U_{max}. The following lemmas show that $u(s) \equiv 0$ implies the corresponding part of the path is a great circular arc and if $u(s) = \pm U_{max}$, the corresponding part of the path is a small circular arc, i.e., arc of radius r.

Lemma 4.0.2. *(i) If for all $s \in [a,b)$, $u(s) \equiv 0$, then the corresponding part of the path is an arc of the great circle.*

(ii) If for all $s \in [a,b)$, $u(s) = U$ with $|U| = U_{max}$, then the corresponding part of the path is a small circular arc of radius r.

Proof. (i) This can be seen from the governing equations:

$$\frac{dX}{ds} = T(s), \qquad \frac{dT}{ds} = -X(s), \qquad \frac{dN}{ds} = 0.$$

Hence, $N(s) = N_0$ is the normal to the plane containing the great circle, and

$$X(s) = \begin{pmatrix} \cos(s) \\ -\sin(s) \\ 0 \end{pmatrix}, \qquad T(s) = \begin{pmatrix} -\sin(s) \\ -\cos(s) \\ 0 \end{pmatrix}. \tag{4.8}$$

(ii) Define $\tilde{X}(s) := u(s)X(s) + N(s)$. For $s \in [a, b)$, we note that $\frac{d\tilde{X}(s)}{ds} = U\frac{dX}{ds} + \frac{dN}{ds} = 0$. Hence, $\tilde{X}(s)$ remains constant on $[a, b)$.

Note that $< \tilde{X}(s), T(s) >= 0$; define $\tilde{N}(s) = \tilde{X}(s) \times T(s) = UN(s) - X(s)$. Then:

$$\frac{d\tilde{X}}{ds} = 0, \qquad \frac{dT(s)}{ds} = \tilde{N}(s), \qquad \frac{d\tilde{N}(s)}{ds} = -(1 + U^2)T(s).$$

Clearly, then

$$\tilde{X}(s) = \tilde{X}(a), \tag{4.9}$$

$$T(s) = T(a)\cos(s\sqrt{1+U^2}) + \tilde{N}(a)\sin(s\sqrt{1+U^2}) \tag{4.10}$$

$$\tilde{N}(s) = \sqrt{1+U^2}[-T(a)\sin(s\sqrt{1+U^2}) + \tilde{N}(a)\cos(s\sqrt{1+U^2})]. \tag{4.11}$$

Clearly, the motion is periodic and the length of the period (circumference of the smaller circle) is $\frac{2\pi}{\sqrt{1+U^2}}$. The motion of the object corresponding to $s \in [a, b)$ is a circular arc of radius $r = \frac{1}{\sqrt{1+U^2}}$ and is in the plane with a normal $\tilde{X}(a)$.

■

Remark. Note that $u(s)$ is the geodesic curvature of the path at s; hence, $u(s) \equiv 0$ corresponds to a great circular arc.

Remark. From the earlier two lemmas, it follows that the optimal path can only consist of great circular arcs or small circular arcs.

If we write $A'(s)$ for $\frac{dA}{ds}$, $B'(s)$ for $\frac{dB}{ds}$ and $C'(s)$ for $\frac{dC}{ds}$, then

$$\begin{pmatrix} A'(s) \\ B'(s) \\ C'(s) \end{pmatrix} = \underbrace{\begin{pmatrix} 0 & 1 & 0 \\ -1 & 0 & u(s) \\ 0 & -u(s) & 0 \end{pmatrix}}_{\Omega(s)} \begin{pmatrix} A(s) \\ B(s) \\ C(s) \end{pmatrix}.$$

Since $u(s)$ is piecewise constant, say on $[s_i, s_{i+1})$, we can express $\Omega_i = \Omega(s)$ on $[s_i, s_{i+1})$ and

$$\begin{pmatrix} A(s) \\ B(s) \\ C(s) \end{pmatrix} = e^{\Omega_i(s-s_i)} \begin{pmatrix} A(s_i) \\ B(s_i) \\ C(s_i) \end{pmatrix}, \quad \forall s \in [s_i, s_{i+1}).$$

Since Ω_i is skew-symmetric, $e^{\Omega_i s}$ is unitary and hence,

$$A^2(s) + B^2(s) + C^2(s) = A^2(s_i) + B^2(s_i) + C^2(s_i), \quad \forall s \in [s_i, s_{i+1}).$$

If $u(s) = U$ on $[s_i, s_{i+1})$, the Darboux/axial vector of Ω_i is given by

$$\begin{pmatrix} k_x \\ k_y \\ k_z \end{pmatrix} = \frac{1}{\sqrt{1+U^2}} \begin{pmatrix} U \\ 0 \\ 1 \end{pmatrix} = \begin{pmatrix} \pm\sqrt{1-r^2} \\ 0 \\ r \end{pmatrix}.$$

If we define $\phi = (s - s_i)\sqrt{1+U^2}$, then

$$e^{\Omega_i(s-s_i)} = I + \hat{\Omega}\sin\phi + \hat{\Omega}^2(1-\cos\phi).$$

Where,

$$I = \begin{pmatrix} 1 & 0 & 0 \\ 0 & 1 & 0 \\ 0 & 0 & 0 \end{pmatrix} \quad \hat{\Omega} = \begin{pmatrix} 0 & -k_z & 0 \\ k_z & 0 & -k_x \\ 0 & k_x & 0 \end{pmatrix} \tag{4.12}$$

Let us turn our attention to inflection points on the spherical path. Inflection occurs when the control input (geodesic curvature) switches from one value to another. If inflection in the optimal path occurs at $s = s_0$, then $u(s)$ is piecewise constant on $(s_0 - \epsilon, s_0)$ and $(s_0, s_0 + \epsilon)$ for sufficiently small $\epsilon > 0$.

Lemma 4.0.3. *If inflexion occurs at $s = s_0$ on the optimal path, then $C(s_0) = -1$ and $A(s_0) = 0$. Furthermore, if s_1, s_2 are consecutive inflexion points with $u(s) = U \in \{U_{max}, -U_{max}\}$ on $[s_1, s_2)$, then $s_2 - s_1 \geq \pi r$.*

Proof. Since $A(s), B(s), C(s)$ are solutions of the ordinary differential equation (4.4), they are continuous in s. From Pontryagin's minimum principle,

$$H(s) = 1 + C(s) + u(s)A(s) \equiv 0.$$

Consider an inflection point, s_0. Then, for $\epsilon > 0$, let $u = u_1$ on $(s_0 - \epsilon)$ and $u = u_2$ on $(s_0, s_0 + \epsilon)$. Then, by Pontryagin's minimum principle,

$$H(s_0 - \epsilon) = 1 + C(s_0 - \epsilon) + u_1 A(s_0 - \epsilon) = 0, \tag{4.13}$$

$$H(s_0 + \epsilon) = 1 + C(s_0 + \epsilon) + u_2 A(s_0 + \epsilon) = 0. \tag{4.14}$$

From continuity, $\lim_{\epsilon \to 0} C(s_0 - \epsilon) = \lim_{\epsilon \to 0} C(s_0 + \epsilon), \quad \lim_{\epsilon \to 0} A(s_0 - \epsilon) = \lim_{\epsilon \to 0} A(s_0 + \epsilon)$. Since $u_1 \neq u_2$, we can conclude that $C(s_0) = -1$, and $A(s_0) = 0$.

On $[s_1, s_2)$, we have

$$\begin{aligned} B'(s) &= -A(s) + UC(s), \\ (-A(s) + UC(s))' &= -B(s) + U(-UB(s)) = -(1+U^2)B(s) \\ \implies B''(s) &= -(1+U^2)B(s). \end{aligned}$$

Hence, if we define $\phi(s) := \sqrt{1+U^2}(s - s_1)$ on $[s_1, s_2)$, we have:

$$\begin{aligned} B(s) &= B(s_1)\cos(\phi(s)) + \frac{-A(s_1) + UC(s_1)}{\sqrt{1+U^2}}\sin(\phi(s)), \\ &= B(s_1)\cos(\phi(s)) - \frac{U}{\sqrt{1+U^2}}\sin(\phi(s)), \\ A(s) &= \frac{1}{\sqrt{1+U^2}}[B(s_1)\sin(\phi(s)) - \frac{U}{1+U^2}(1-\cos(\phi(s)))]. \end{aligned}$$

From Pontryagin's minimum principle, $UA(s) \leq 0$ for $s \in [s_1, s_2)$; hence,

$$UB(s_1)\sin(\phi(s)) - \frac{U^2}{1+U^2}(1-\cos(\phi(s))) \leq 0.$$

To prove the second part, we note that $A(s_1) = 0, A(s_2) = 0$; by Rolle's Theorem, there is a $\bar{s} \in (s_1, s_2)$ such that $B(\bar{s}) = A'(\bar{s}) = 0$. But,

$$B(\bar{s}) = 0 \implies B(s_1)\cos(\phi(\bar{s})) - \frac{U}{\sqrt{1+U^2}}\sin(\phi(\bar{s})) = 0.$$

If $\cos(\phi(\bar{s}))) \neq 0$,

$$\begin{aligned} & U\sin(\phi(\bar{s}))[\frac{U}{\sqrt{1+U^2}}\tan(\phi(\bar{s}))] - \frac{U^2}{1+U^2}(1-\cos(\phi(\bar{s})) \leq 0. \\ & \implies \sqrt{1+U^2}\sin(\phi(\bar{s}))\tan(\phi(\bar{s})) - (1-\cos\phi(\bar{s})) \leq 0. \\ & \sqrt{1+U^2}\frac{(1+\cos\phi(\bar{s}))}{\cos\phi(\bar{s})} - 1 \leq 0 \implies \frac{1+\cos\phi(\bar{s})}{\cos\phi(\bar{s})} \leq \frac{1}{\sqrt{1+U^2}} = r < 1. \end{aligned} \tag{4.15}$$

This implies that $\cos\phi(\bar{s}) < 0$. It suffices to show that $\bar{s} = \frac{1}{2}(s_1 + s_2)$ to arrive at the desired result.

Note that

$$\begin{aligned} A(s) &= \frac{1}{\sqrt{1+U^2}}[B(s_1)\sin(\phi(s)) - \frac{U}{1+U^2}(1-\cos(\phi(s)))], \\ A(s_i) &= \frac{1}{\sqrt{1+U^2}}[B(s_1)\sin(\phi(s_i)) - \frac{U}{1+U^2}(1-\cos(\phi(s_i)))] = 0, \quad i = 1, 2. \\ \implies & \quad B(s_1)[\sin\phi(s_2) - \sin\phi(s_1)] - \frac{U}{1+U^2}(\cos\phi(s_1) - \cos\phi(s_2))] = 0, \\ \implies & \quad B(s_1)\cos\left(\phi\left(\frac{s_1+s_2}{2}\right)\right) - \frac{U}{1+U^2}\sin\left(\phi\left(\frac{s_1+s_2}{2}\right)\right) = 0. \end{aligned}$$

Note that $s_2 - s_1 \leq 2\pi r$ as the path would be non-optimal otherwise. Since $\phi(\frac{s_1+s_2}{2}) = \sqrt{1+U^2}(\frac{s_2-s_1}{2}) = \frac{s_2-s_1}{2r} \leq \pi$, it follows that $\bar{s} = \frac{s_1+s_2}{2}$ as it is the only solution for $B(s) = 0$ in the interval $[s_1, s_2)$. Since $\cos(\phi(\bar{s})) < 0$, it implies that $\phi(\bar{s}) = \frac{s_2-s_1}{2r} \in (\frac{\pi}{2}, \frac{3\pi}{2})$; given that $s_2 - s_1 \leq 2\pi r$, this implies that $\frac{s_2-s_1}{2r} \in (\frac{\pi}{2}, \pi)$; in other words, $2\pi r > s_2 - s_1 \geq \pi r$ ■

Lemma 4.0.4. *Suppose a great circular arc is part of an optimal path. Then* $A^2(s) + B^2(s) + C^2(s) = 1$ *throughout the path.*

Proof. Let the geodesic curvature be piecewise constant; in particular, say $u(s) = U_i$ on $[s_i, s_{i+1})$. We have seen before that if $u(s) = U_i$, a constant on $[s_i, s_{i+1})$, then $A^2(s) + B^2(s) + C^2(s) = A^2(s_i) + B^2(s_i) + C^2(s_i)$ for all $s \in [s_i, s_{i+1})$. By continuity of $A(s), B(s), C(s)$, it follows that $A^2(s) + B^2(s) + C^2(s)$ must be the same constant throughout the path, i.e., for every i, we have $A^2(s_i)+B^2(s_i)+C^2(s_i)$ must be the same. It then suffices to show that $A^2(s_i)+B^2(s_i)+C^2(s_i) = 1$ at some inflexion point.

Note that if $u = U$, a constant, then the corresponding path will be a circular arc of radius $\frac{1}{\sqrt{1+U^2}}$; hence, if great circular arc is part of an optimal path, then $u(s) \equiv 0$ on $[s_i, s_{i+1})$ for some i. We also know, from the earlier Lemma, that $C(s_i) = -1$ and $A(s_i) = 0$. Since $u(s) \equiv 0$ on $[s_i, s_{i+1})$ (otherwise, the path cannot be a greater circular arc), we must also have $A(s) \equiv 0$ (otherwise, by Pontryagin's minimum principle, we must have $u(s) = \pm U_{max}$, which would not correspond to a great circle. From equations (4.4), it follows that $B(s) \equiv 0$ for $s \in [s_i, s_{i+1})$; in particular, $B(s_i). = 0$ and hence, $A^2(s_i) + B^2(s_i) + C^2(s_i) = 1$, implying that $A^2(s) + B^2(s) +$

$C^2(s) \equiv 1$ throughout the path. ■

We will show that if $r \in (0, \frac{1}{2}]$, the optimal path consists of at most three segments; more specifically, optimal path must be of the form CGC or CCC or a subpath of these. This is a direct generalization of the Dubins result for the planar case to the spherical case.

As in the planar case, one can consider the types of paths with at most four segments with no two G segments being contiguous: (1) CCCC, (2)CCCG, (3) CCGC, (4) CGCC, (5) GCCC, (6) CGCG, (7) GCGC, (8) GCCG. Non-contiguity of two greater circular arcs limits the paths to contain at most two of them in a path consisting of four segments. It then suffices to show that GCG, GCC and CCCC paths are not optimal to rule out possibility of optimality of any path expressible as a concatenation of four or more segments. We will first begin by showing that GCG and GCC paths are not optimal:

Lemma 4.0.5. *Any non-trivial GCG and GCC paths are not optimal.*

Proof. A non-trivial path consists of arcs of non-zero length. Note that a GCG path contains a great circular arc, and consequently, $A^2(s) + B^2(s) + C^2(s) \equiv 1$ throughout the path. Let the two inflexion points be s_1 and s_2 and the smaller circular arc corresponds to $s \in [s_1, s_2)$. Since s_1, s_2 are inflexion points, we know that $A(s_1) = 0, C(s_1) = -1$; similarly, $A(s_2) = 0, C(s_2) = -1$. This also implies that $B(s_1) = 0$ and $B(s_2) = 0$ as $A^2(s_1)+B^2(s_1)+C^2(s_1) = A^2(s_2)+B^2(s_2)+C^2(s_2) = 1$. Since $u(s) = U_2 \neq 0$ on $[s_1, s_2)$ as it corresponds to a smaller circular arc, we know that

$$\begin{pmatrix} A(s_2) \\ B(s_2) \\ C(s_2) \end{pmatrix} = e^{\Omega_1(s_2-s_1)} \begin{pmatrix} A(s_1) \\ B(s_1) \\ C(s_1) \end{pmatrix}. \tag{4.16}$$

Equivalently,

$$\underbrace{\begin{pmatrix} 0 \\ 0 \\ -1 \end{pmatrix}}_{\mathbf{w}} = e^{\Omega_1(s_2-s_1)} \underbrace{\begin{pmatrix} 0 \\ 0 \\ -1 \end{pmatrix}}_{\mathbf{w}}. \tag{4.17}$$

This means that either $\mathbf{w}$ is an axial vector of Ω_2 or $s_2 = s_1$. But neither of them is true, as the former would mean $r = 1$ and the latter would imply triviality of the GCG path. Hence, any non-trivial GCG path cannot be optimal.

A similar reasoning holds for the GCC path. ■

The next theorem completes the characterization of Dubins paths on a sphere:

Theorem 4.0.6. *If $0 < r \leq \frac{1}{2}$, then any non-trivial CCCC path cannot be optimal.*

The proof of this theorem is accomplished in the following steps:

- First we show that the second and third circular arc lengths are equal and exceed the semi-perimeter (i.e., are of length greater than πr). This is shown in Lemma 4.0.8.
- We then show that a CCC path with the last circular arcs of the same length and exceeding semi-perimeter in length cannot be optimal if $0 < r \leq \frac{1}{2}$.

Lemma 4.0.7. *If a non-trivial CCCC path were to be optimal, then the middle arcs must be of the same length exceeding πr.*

Proof. Let the length of the CCCC path be L, with each segment corresponding to one of the four intervals $[s_0, s_1), [s_1, s_2), [s_2, s_3), [s_3, s_4)$, with $s_0 = 0, \quad s_4 = L$. The control input on the interval $[s_i, s_{i+1})$ is u_i, with $u_i = (-1)^{i-1}U$. Define

$$\Omega_1 = \begin{pmatrix} 0 & 1 & 0 \\ -1 & 0 & U \\ 0 & -U & 0 \end{pmatrix}, \quad \Omega_2 = \begin{pmatrix} 0 & 1 & 0 \\ -1 & 0 & -U \\ 0 & U & 0 \end{pmatrix}.$$

Note that s_1, s_2, s_3 are inflexion points. Define $\phi_1 := s_1\sqrt{1+U^2}, \quad \phi_2 := (s_2 - s_1)\sqrt{1+U^2}, \quad \phi_3 := (s_3 - s_2)\sqrt{1+U^2}, \quad \phi_4 := (s_4 - s_3)\sqrt{1+U^2}$. Note that $\phi_1, \phi_2, \phi_3, \phi_4$ are the angles subtended at their respective centers by the four circular arcs in the CCCC path; since the circular arcs are of the same radius, it suffices to show that $\phi_2 = \phi_3$.

Since great circular arc is not part of the CCCC path, let $B(s_1) = B_0 \neq 0$; correspondingly

$$A^2(s) + B^2(s) + C^2(s) = 1 + B_0^2.$$

At an inflexion point, s_i, we have $A(s_i) = 0$ and $C(s_i) = -1$. Hence, at any inflexion point, we must have $B(s_i) = \pm B_0$. Hence, at s_2 and s_3, we must have:

$$\begin{pmatrix} A(s_2) \\ B(s_2) \\ C(s_2) \end{pmatrix}, \begin{pmatrix} A(s_3) \\ B(s_3) \\ C(s_3) \end{pmatrix} \in \{ \begin{pmatrix} 0 \\ B_0 \\ -1 \end{pmatrix}, \begin{pmatrix} 0 \\ -B_0 \\ -1 \end{pmatrix} \}.$$

Consider the inflexion point s_2; suppose

$$\begin{pmatrix} A(s_2) \\ B(s_2) \\ C(s_2) \end{pmatrix} = \underbrace{\begin{pmatrix} 0 \\ B_0 \\ -1 \end{pmatrix}}_{\mathbf{u}_1}. \tag{4.18}$$

However, this would imply

$$\mathbf{u}_1 = e^{\Omega_1(s_2 - s_1)}\mathbf{u}_1.$$

In other words, $\mathbf{u}_1$ must be the axial vector of Ω_1 or $s_2 - s_1 = 0$; neither of them is true - the former is not true because the axial vector of Ω_1 is $\begin{pmatrix} \sqrt{1-r^2} \\ 0 \\ r \end{pmatrix}$; the latter is not true because the

trajectory is non-trivial. Hence,

$$\begin{pmatrix} A(s_2) \\ B(s_2) \\ C(s_2) \end{pmatrix} = \underbrace{\begin{pmatrix} 0 \\ -B_0 \\ -1 \end{pmatrix}}_{\mathbf{u}_2}. \tag{4.19}$$

Consider the inflexion point s_3. By the same reasoning as that for inflexion point s_2, we must have

$$\begin{pmatrix} A(s_3) \\ B(s_3) \\ C(s_3) \end{pmatrix} = \begin{pmatrix} 0 \\ B_0 \\ -1 \end{pmatrix}. \tag{4.20}$$

However, this would imply that

$$\mathbf{u}_2 = e^{\Omega_1(s_2-s_1)}\mathbf{u}_1, \quad \mathbf{u}_1 = e^{\Omega_2(s_3-s_2)}\mathbf{u}_2.$$

Combining,

$$e^{\Omega_1(s_2-s_1)}\mathbf{u}_1 = e^{-\Omega_2(s_3-s_2)}\mathbf{u}_1 \implies [e^{\Omega_1(s_2-s_1)} - e^{-\Omega_2(s_3-s_2)}]\mathbf{u}_1 = 0.$$

If we define $\hat{\Omega}_1 = \frac{1}{\sqrt{1+U_{max}^2}}\Omega_1$ and $\hat{\Omega}_2 = \frac{1}{\sqrt{1+U_{max}^2}}\Omega_2$, then,

$$e^{\Omega_1(s_2-s_1)} = e^{\hat{\Omega}_1\phi_2}, \quad e^{\Omega_2(s_3-s_2)} = e^{\hat{\Omega}_2\phi_3}$$

implying

$$[e^{\hat{\Omega}_1\phi_2} - e^{-\hat{\Omega}_2\phi_3}]\mathbf{u}_1 = 0.$$

Using Euler-Rodriguez formula for exponential of a skew-symmetric matrix,

Denote for compactness:

$$L = \cos\phi_2 - \cos\phi_3; \quad M = \sin\phi_2 + \sin\phi_3; \quad N = -\cos\phi_2 - \cos\phi_3;$$
$$Q = \sin\phi_2 - \sin\phi_3$$

$$[e^{\hat{\Omega}_1\phi_2} - e^{\hat{\Omega}_2\phi_3}] = \begin{pmatrix} r^2L & -rM & r\sqrt{1-r^2}(2+N) \\ rM & L & -\sqrt{1-r^2}Q \\ r\sqrt{1-r^2}(2+N) & \sqrt{1-r^2}Q & (1-r^2)L \end{pmatrix}$$

Since

$$[e^{\hat{\Omega}_1\phi_2} - e^{-\hat{\Omega}_2\phi_3}]\mathbf{u}_1 = 0,$$

implies, upon simplification,

$$B_0 \begin{pmatrix} -rM \\ L \\ \sqrt{1-r^2}Q \end{pmatrix} - \sqrt{1-r^2} \begin{pmatrix} r(2+N) \\ -Q \\ \sqrt{1-r^2}L \end{pmatrix} = \begin{pmatrix} 0 \\ 0 \\ 0 \end{pmatrix}. \tag{4.21}$$

The last two equations of the above system of equations can be expressed as:

$$\begin{pmatrix} \frac{B_0}{\sqrt{1-r^2}} & 1 \\ -1 & \frac{B_0}{\sqrt{1-r^2}} \end{pmatrix} \begin{pmatrix} \cos\phi_2 - \cos\phi_3 \\ \sin\phi_2 - \sin\phi_3 \end{pmatrix} = \begin{pmatrix} 0 \\ 0 \end{pmatrix} \tag{4.22}$$

Since the determinant of the 2×2 matrix on the left hand side is $1 + \frac{B_0^2}{1-r^2} > 0$, it follows that $\cos\phi_2 = \cos\phi_3$ and $\sin\phi_2 = \sin\phi_3$ implying that $\phi_2 = \phi_3$.

To prove the theorem, it is necessary to distinguish a circular arc by its orientation, i.e., whether $u(s) = U_{max}$ or $u(s) = -U_{max}$. An arc, C, is of type L if corresponding $u(s) = U_{max}$ and of type R if corresponding $u(s) = -U_{max}$. Hence, we can be more specific and distinguish between concatenations; for example, while LGR, LGL, RGL, RGR are all paths of type CGC, they are

clearly four different paths.

If we had a non-trivial CCCC path, it can be of type LRLR or RLRL; optimality of path necessitates that two central arcs have arc lengths exceeding πr and be equal. To show non-optimality, it suffices to consider non-optimality of paths of type LRLR (and by reflection symmetry, the result also holds for RLRL). To show non-optimality of LRLR, it suffices to show that a subpath of LRLR consisting of only three segments is non-optimal. Consider a subpath consisting of a sufficiently small piece of the first L arc concatenated with the second and third arcs. Let the angle of the first arc be $\alpha << 1$ while the second and third arcs be $\pi + \phi$, with $0 < \phi < \pi$. We will show that this path is non-optimal if $0 < r \leq \frac{1}{2}$ to conclude the proof of Theorem 2.

Lemma 4.0.8. *Consider an LRL path with the first arc angle being α and the latter two being $\pi+\phi$ with $\phi \in (0, \pi)$ and $r \in (0, \frac{1}{2}]$. Then, there is a path of type RLR with smaller length, implying its non-optimality.*

Proof. Since $\alpha << 1$, we may use regular perturbation technique. It is easier to see that angles corresponding to arcs in the RLR paths may be chosen to be $\pi + \phi + \xi(\alpha), \pi + \phi + \eta(\alpha)$ and $\beta(\alpha)$ respectively. Note that the angles $\xi(\alpha), \eta(\alpha), \beta(\alpha)$ are all expressed as functions of the perturbation variable α. In what follows, the following symbols are used:

$$R_L(\theta) = I + \Omega_L \sin\theta + \Omega_L^2(1 - \cos\theta)$$
$$R_R(\theta) = I + \Omega_R \sin\theta + \Omega_R^2(1 - \cos\theta)$$

The above definitions refer to the Rodrigues' rotation formulae about axes $\mathbf{u}_L, \mathbf{u}_R$ respectively. Where $\mathbf{u}_L, \mathbf{u}_R$ refer to axes about which left and right turns are performed respectively and are defined as:

$$\mathbf{u}_L = \begin{pmatrix} \sqrt{1-r^2} \\ 0 \\ r \end{pmatrix}, \qquad \mathbf{u}_R = \begin{pmatrix} -\sqrt{1-r^2} \\ 0 \\ r \end{pmatrix}$$

Ω_L, Ω_R are the corresponding unique skew-symmetric matrices associated with the axes about

which the turns occur ($\mathbf{u}_L$ and $\mathbf{u}_R$ respectively). If the CCC sub-path considered is of type LRL, the following equation must hold for sufficiently small α since the initial and final configurations remain the same but the paths being compared vary:

$$R_L(\alpha)R_R(\pi+\phi)R_L(\pi+\phi) = R_R(\pi+\phi+\xi(\alpha))R_L(\pi+\phi+\eta(\alpha))R_R(\beta(\alpha)) \tag{4.23}$$

Clearly, when $\alpha = 0, \xi(0) = 0, \eta(0) = 0$ and $\beta(0) = 0$ will ensure that the default case considered is the CC path with angles $(\pi+\phi)$ for both arcs. This default case can be interpreted as a CCC path with the first angle $\alpha = 0$. α being the variable which is then perturbed in order to show that the CCC sub-path is longer. Denote:

$$a_1 = \left.\frac{d\xi(\alpha)}{d\alpha}\right|_{\alpha=0}, \qquad a_2 = \left.\frac{d\eta(\alpha)}{d\alpha}\right|_{\alpha=0}, \qquad a_3 = \left.\frac{d\beta(\alpha)}{d\alpha}\right|_{\alpha=0} \tag{4.24}$$

Differentiating equation 4.23 with respect to the perturbation variable α and evaluating at the default case,

$$\begin{aligned}\Omega_L R_L(\alpha)R_R(\pi+\phi)R_L(\pi+\phi) &= a_1\Omega_R R_R(\pi+\phi)R_L(\pi+\phi) \\ &+ a_2 R_R(\pi+\phi)R_L(\pi+\phi)\Omega_L + a_3 R_R(\pi+\phi)R_L(\pi+\phi)\Omega_R\end{aligned} \tag{4.25}$$

The condition for the RLR path to be shorter than the LRL path is as follows:

$$\alpha+\pi+\phi+\pi+\phi > \pi+\phi+\xi(\alpha)+\pi+\phi+\eta(\alpha)+\beta(\alpha) \tag{4.26}$$

Differentiating the above with respect to α and evaluating at $\alpha = 0$,

$$1 > a_1 + a_2 + a_3 \tag{4.27}$$

Solving for a_1, a_2, a_3 using equation 4.25, 3 equations in a_1, a_2, a_3 are arrived at using the following

operations:

$$\mathbf{u}_L^*(\text{LHS})\mathbf{u}_R = \mathbf{u}_L^*(\text{RHS})\mathbf{u}_R \tag{4.28}$$

$$\mathbf{u}_R^*(\text{LHS})\mathbf{u}_L = \mathbf{u}_R^*(\text{RHS})\mathbf{u}_L \tag{4.29}$$

$$\mathbf{u}_R^*(\text{LHS})\mathbf{u}_R = \mathbf{u}_R^*(\text{RHS})\mathbf{u}_R \tag{4.30}$$

Upon solving equations 4.28, 4.29, 4.30; a_1, a_2, a_3 are determined to be:

$$a_1 = \cos\phi - (1-2r^2)(1+\cos\phi); \quad a_2 = -a_1 = -[\cos\phi - (1-2r^2)(1+\cos\phi)]$$

$$a_3 = 1$$

Thus,

$$a_1 + a_2 + a_3 = 1$$

Comparing the above with condition 4.27, it is evident that the first order Taylor's series expansion coefficients are not sufficient to show the non-optimality of the CCC sub-path and that the second order coefficients must be computed. In computing the second order Taylor's series expansion coefficients, denote:

$$b_1 = \frac{d^2\xi(\alpha)}{d\alpha^2}\bigg|_{\alpha=0}, \qquad b_2 = \frac{d^2\eta(\alpha)}{d\alpha^2}\bigg|_{\alpha=0}, \qquad b_3 = \frac{d^2\beta(\alpha)}{d\alpha^2}\bigg|_{\alpha=0} \tag{4.31}$$

The condition for the LRL subpath to be non-optimal in second order Taylor's series expansion coefficients is obtained by differentiating 4.26 twice with respect to α to get:

$$b_1 + b_2 + b_3 < 0 \tag{4.32}$$

The following equation is arrived at upon differentiating equation 4.25 with respect to α:

$$\begin{aligned}
&\Omega_L^2 R_R(\pi+\phi)R_L(\pi+\phi) \\
&= b_1[\Omega_R R_R(\pi+\phi)R_L(\pi+\phi)] + a_1^2[\Omega_R^2 R_R(\pi+\phi)R_L(\pi+\phi)] \\
&+ a_1a_2[\Omega_R R_R(\pi+\phi)R_L(\pi+\phi)\Omega_L] + a_1a_3[\Omega_R R_R(\pi+\phi)R_L(\pi+\phi)\Omega_R] \\
&+ b_2[R_R(\pi+\phi)R_L(\pi+\phi)\Omega_L] + a_1a_2[\Omega_R R_R(\pi+\phi)R_L(\pi+\phi)\Omega_L] \\
&+ a_2^2[R_R(\pi+\phi)R_L(\pi+\phi)\Omega_L^2] + a_2a_3[R_R(\pi+\phi)R_L(\pi+\phi)\Omega_L\Omega_R] \\
&+ b_3[R_R(\pi+\phi)R_L(\pi+\phi)\Omega_R] + a_1a_3[\Omega_R R_R(\pi+\phi)R_L(\pi+\phi)\Omega_R] \\
&+ a_2a_3[R_R(\pi+\phi)R_L(\pi+\phi)\Omega_L\Omega_R] + a_3^2[R_R(\pi+\phi)R_L(\pi+\phi)\Omega_R^2]
\end{aligned} \tag{4.33}$$

Similar to the first order case, the following operations are used on equation 4.33 above to arrive at 3 equations in b_1, b_2, b_3:

$$\mathbf{u}_L^*(\text{LHS})\mathbf{u}_R = \mathbf{u}_L^*(\text{RHS})\mathbf{u}_R \tag{4.34}$$

$$\mathbf{u}_R^*(\text{LHS})\mathbf{u}_L = \mathbf{u}_R^*(\text{RHS})\mathbf{u}_L \tag{4.35}$$

$$\mathbf{u}_R^*(\text{LHS})\mathbf{u}_R = \mathbf{u}_R^*(\text{RHS})\mathbf{u}_R \tag{4.36}$$

Upon solving equations 4.34, 4.35, 4.36; the following solutions to b values are obtained:

$$\begin{aligned}
b_1 \sin\phi &= 4\cos^3\phi r^4 + \cos^2\phi(4r^4 - 2r^2) + \cos\phi(-4r^4 + 4r^2) - 4r^4 + 6r^2 - 2 \\
b_2 \sin\phi &= -4\cos^3\phi r^4 + \cos^2\phi(-12r^4 + 6r^2) + \cos\phi(-12r^4 + 12r^2 - 2) \\
&\quad - 4r^4 + 6r^2 - 2 \\
b_3 \sin\phi &= 4\cos^2\phi r^2 + \cos\phi(4r^2 - 2)
\end{aligned}$$

As per condition 4.32 mentioned for b (second order Taylor's series expansion coefficients) values, in order to prove non-optimality of the sub-path, the expression $(b_1 + b_2 + b_3)$ must be negative for all $\phi \in (0, \pi)$ and for all $r \in (0, \frac{1}{2}]$. It is evident that in the range of ϕ of current interest, whenever $(b_1 + b_2 + b_3)$ is negative, $(b_1 + b_2 + b_3)\sin\phi$ is also negative since in this range of ϕ values,

$\sin\phi$ is always positive. Hence, the following polynomial for the expression $(b_1 + b_2 + b_3)\sin\phi$ is considered for analysis and it is the aim of the current endeavor to show that this polynomial is negative for all $\phi \in (0, \pi)$ and for all $r \in (0, \frac{1}{2}]$:

$$(b_1 + b_2 + b_3)\sin\phi = \cos^2\phi(-8r^4 + 8r^2) + \cos\phi(-16r^4 + 20r^2 - 4) - 8r^4 + 12r^2 - 4 \quad (4.37)$$

Denote for compactness:

$$\lambda = r^2; \qquad P = \cos\phi$$

Thus, it must be shown that:

$$P^2(-8\lambda^2 + 8\lambda) + P(-16\lambda^2 + 20\lambda - 4) - 8\lambda^2 + 12\lambda - 4 < 0 \quad (4.38)$$

Convert the above polynomial into one in terms of λ so that a range in λ (essentially a range in r) for when the value is negative may be determined. Thus, the required condition 4.38 upon substitution of variables and simplification becomes:

$$F(\lambda) = 2\lambda^2(P + 1) - \lambda(2P + 3) + 1 > 0 \quad (4.39)$$

Since the second derivative of $F(\lambda)$ above is $4(P + 1) > 0$ in the range considered, it is convex. Note that since derivatives exist in the ranges of values considered, the $F(\lambda)$ is continuous and a change in slope from negative to positive value without a minimum being traversed is not possible. Keeping this in mind, in order to show that the $F(\lambda) > 0$ in the intervals $\phi \in (0, \pi)$ (which translates to $P \in (-1, 1)$) and $\lambda \in \left(0, \frac{1}{4}\right]$, the following possibilities are considered:

1. $F'(0) > 0$ and $\min F(\lambda) = F(0) \geq 0$
2. $F'(\lambda) = 0$ for some $\lambda \in \left(0, \frac{1}{4}\right]$ and $\min F(\lambda) \geq 0$
3. $F'\left(\frac{1}{4}\right) < 0$ and $\min F(\lambda) = F\left(\frac{1}{4}\right) \geq 0$

Considering case 1.:

$F'(0) < 0$ and hence is ruled out.

Considering case 2.:

$$F'(\lambda) = 0 \text{ for some } \lambda \in \left(\frac{1}{4}\right]$$
$$\lambda = \frac{(2P+3)}{4(P+1)}; \quad \frac{(2P+3)}{4(P+1)} < \frac{1}{4}; \quad P < -2$$

The above statement, however, is not possible considering the range of P being $(-1, 1)$. Thus, keeping in mind that $F'(0) < 0$ (thus satisfying the first condition since the second case was ruled out), the third case is considered knowing that only the second part of it $\left(F\left(\frac{1}{4}\right) \geq 0\right)$ must be shown:

$$F\left(\frac{1}{4}\right) = 2\left(\frac{1}{4}\right)^2 (P+1) - \left(\frac{1}{4}\right)(2P+3) + 1 = \frac{3-3P}{8} > 0$$

■

■

5. COMPUTATIONAL RESULTS

Python 3 codes was developed using the NumPy, and Math libraries and the Plotly package for visualizing the non-optimality of the $CCCC$ type path traversed by a Dubins' vehicle on a sphere. Only fundamental linear algebraic results were used to perform all the computations. Refer to appendices B and C to see the mathematical basis for the computations, and all the codes respectively.

In the main set of codes developed, the radius of the sphere (R) minimum turning radius of the vehicle (r), initial and final positions (u, v), and the initial and final velocities (U, V) are given as input and the potential optimal paths are plotted along with all geometrical details. First, the possible tight circles are displayed and then, all potential optimal paths are plotted and the relevant data is displayed. Figures 5.1, 5.2, 5.3, and 5.4 are a few illustrations showcasing what the output files are like:

```
R = 100
r = 50
u = [60.5758387 79.33752411 -6.01041038]
v = [-20.21866901 -16.42068107 -96.54826077]
dU = [[ 67.65415539 45.13242784 29.76540299] [ 23.20960266 73.87385833 -38.78101855]]
dV = [[ 24.80126709 0.57711498 -82.97327334] [-55.1292706 -25.20813659 -61.84911781]]
U = [-0.60801399 0.51030685 0.60819891]
V = [-0.32751859 0.94041776 -0.09135649]
```

Figure 5.1: Data of Possible Tight Circles

In the secondary code developed, a CCC sub-path of a CCCC type path is constructed and then the initial and final positions and velocities are sent to the main set of codes to find the potential optimal paths. This is a reasonable approach since if a sub-path of a particular type of path is non-optimal, then the path itself cannot be optimal.

Following the results of Lemma 4.0.7. in the previous section, the sub-path was constructed was a $C_\alpha C_{\pi+\phi} C_{\pi+\phi}$ type path. With the secondary code, keeping a constant value of $\alpha = 1°$, ϕ values were run through from $\phi = 2°$ to $\phi = 178°$ in increments of $2°$, and r values were run

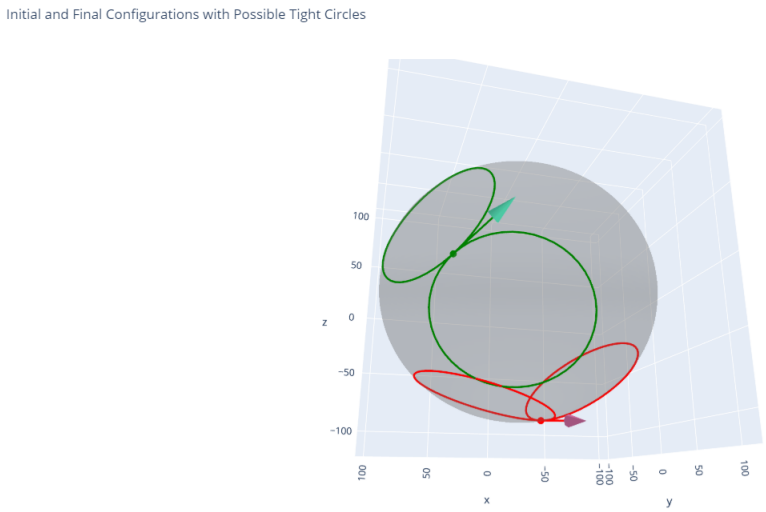

Figure 5.2: Plot of Possible Tight Circles

GC Path:Direct Tangent Plane
Initial Tight Circle = [67.65415539 45.13242784 29.76540299]
Final Tight Circle = [24.80126709 0.57711498 -82.97327334]
Angle1 (Initial TC) in degrees = 80.53037476830534
Angle2 (Tangent GC) in degrees = 242.0
Angle3 (Final TC) in degrees = 321.5303747683053
Distance = 773.2338726051339
Tangent Point 1 = [36.50316956 75.92765555 53.87494534]
Tangent Point 2 = [-20.63401485 16.52057173 -96.44328977]

Figure 5.3: Data of a Potential Optimal Path

through from 1 to 99 in increments of 1 with an R value kept constant at 100. This means that a total of 8900 cases were run to generate the following plots which characterize the nature of optimality.

Before this, computation was done keeping a constant value of $\alpha = 1°$, ϕ values were run through from $\phi = 2°$ to $\phi = 178°$ in increments of $2°$, with $r = \frac{1}{\sqrt{2}}$ and $R = 1$. This was done first since [2] has shown that for $r = \frac{1}{\sqrt{2}}$, a $C_\alpha C_{\pi+\phi} C_{\pi+\phi}$ type path cannot be optimal. The code's computational results were in line with this proven result and can be seen in plots 5.5 and 5.6.

The plots corresponding to the computational results in agreement with the main result of this work are then shown in figure 5.7 which shows that the results of Lemma 4.0.8. are valid, and in

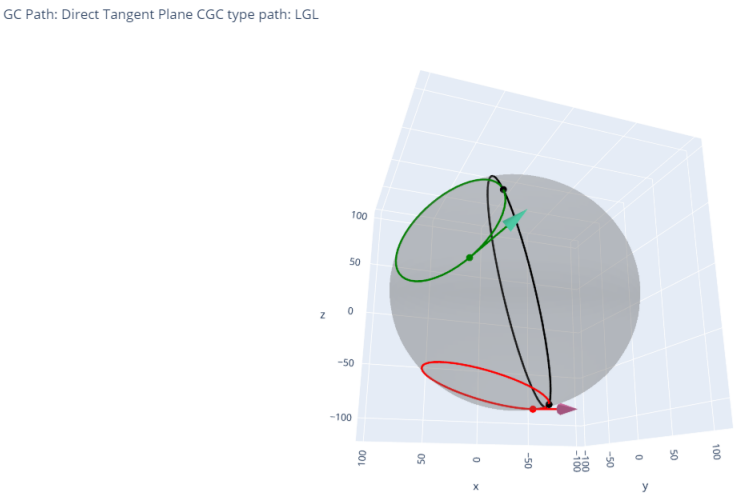

Figure 5.4: Plot of a Potential Optimal Path

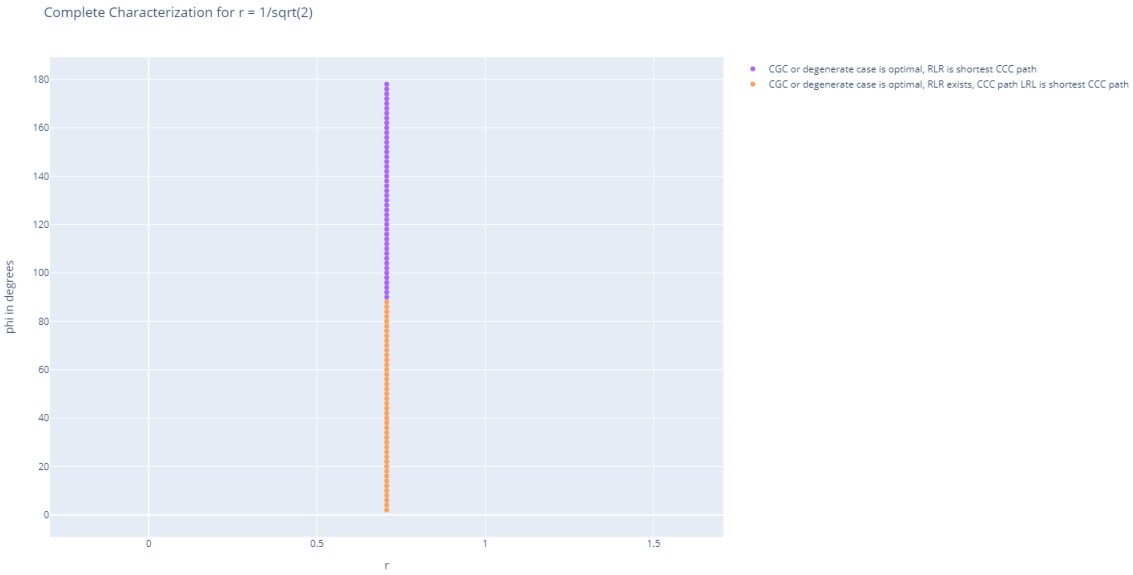

Figure 5.5: Complete Characterization for $r = \frac{1}{\sqrt{2}}$

figure 5.8 which shows the main result of this proof.

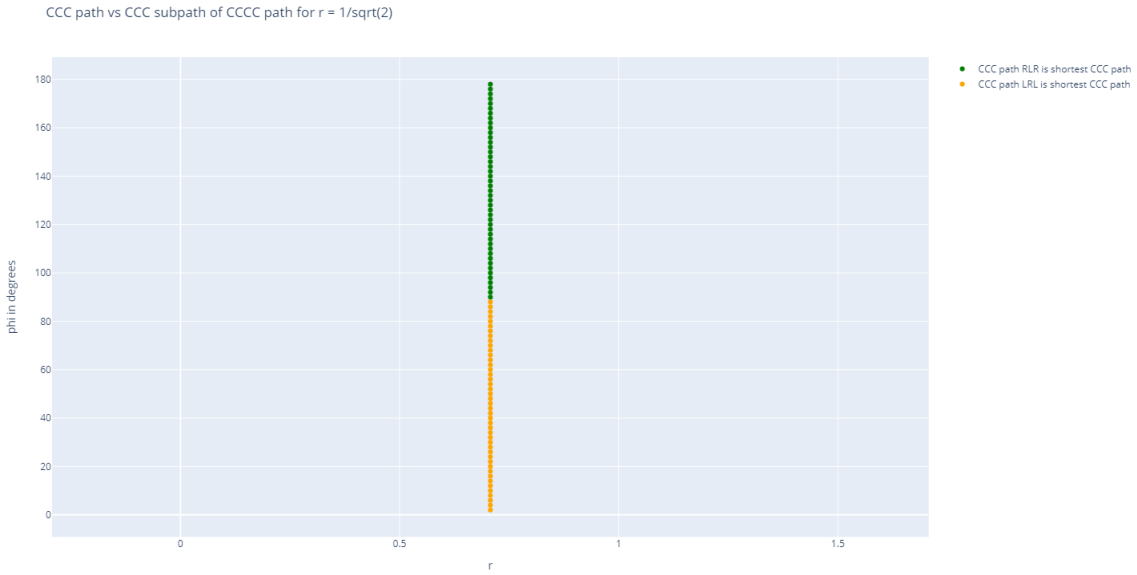

Figure 5.6: Comparing only CCC Paths for $r = \frac{1}{\sqrt{2}}$

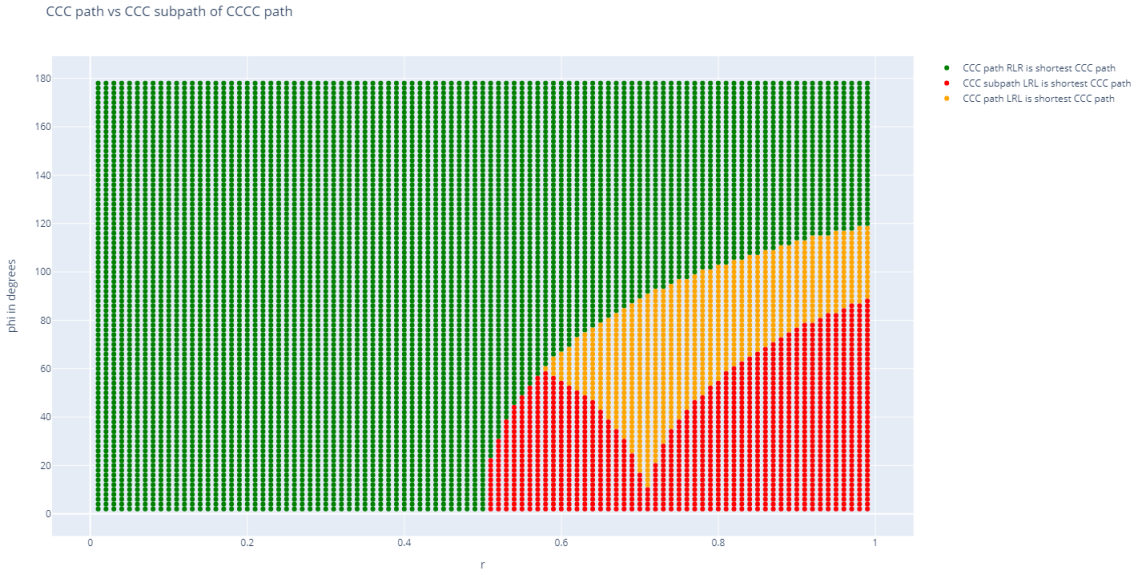

Figure 5.7: Comparing only CCC Paths

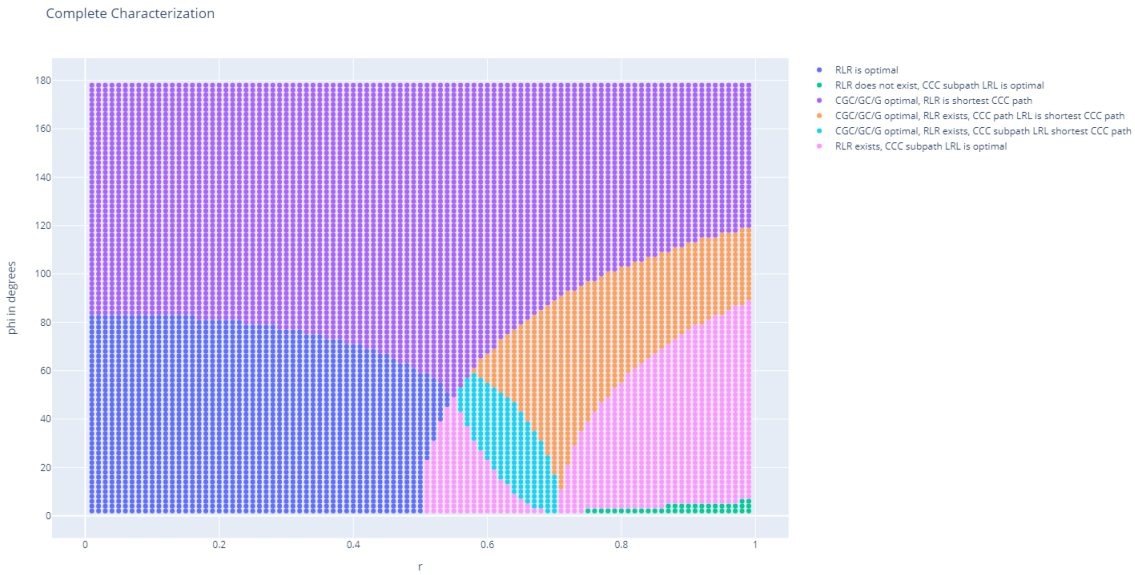

Figure 5.8: Complete Characterization

6. CONCLUSIONS AND DISCUSSION

Through the computational results obtained, which have been discussed in the previous section, it is found that for $r \in \left(0, \frac{1}{2}\right]$, at least one Dubins' type path is shorter than the CCC sub-path (of the CCCC path) construction. In other words, only the Dubins' type paths can be optimal for $r \in (0, \frac{1}{2}]$. This is in line with the main result of this work which was shown to be true analytically.

Note how in 5.8, the case when $r = \frac{1}{\sqrt{2}}$ appears to be a singularity and even a slight disturbance to the r value about that point seems to cause a non-trivial $CCCC$ to be optimal. This result makes sense intuitively as it is not possible to have Dubins' type paths as r increases due to a decrease in maneuverability on the sphere. This phenomenon of Dubins' type paths being infeasible is very clearly illustrated by the extreme case shown in figure 6.1 in which the initial and final positions are the same (u=v), and the initial and final velocities are opposite in nature (U=-V).

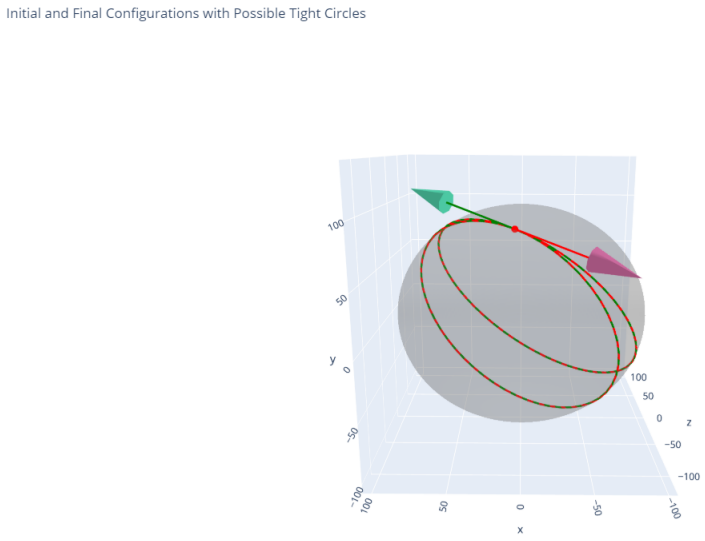

Figure 6.1: No Dubins' Type Path Exists: u=v, U=-V, r=0.99

The plot comparing only CCC paths, 5.7, was checked against the values of zeros obtained

from plots of the polynomial obtained for the second order Taylor's series expansion coefficients, 4.37, and the values at which changes in optimality occurred were in agreement till before the yellow region begins. Once the yellow region begins, the zeros are in agreement with the line separating the yellow and green regions. However, this is enough to demonstrate that the $CCCC$ path is definitely not optimal for $r \in \left(0, \frac{1}{2}\right]$. The plot of polynomial 4.37 when the $C_\alpha C_{\pi+\phi} C_{\pi+\phi}$

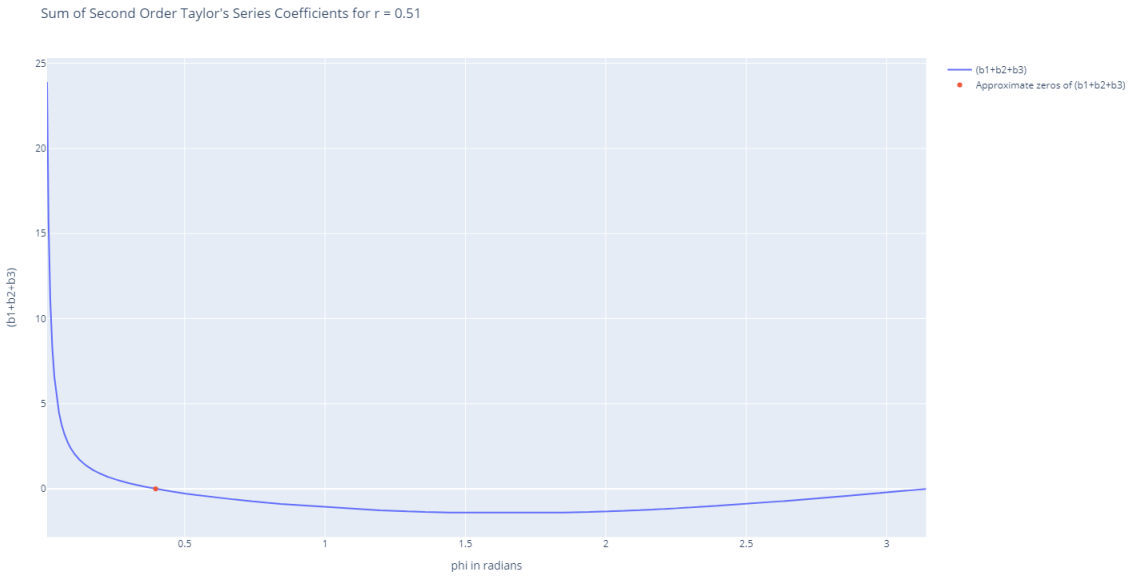

Figure 6.2: Second Order Taylor's Series Expansion Coefficients at $r = 0.51$

path becomes optimal (at $r = 0.51$), figure 6.2, is shown. Also note that there is good agreement between the zero of the polynomial 4.37 evaluated at $r = \frac{1}{\sqrt{2}}$ and the plot 5.6. The plot figure 6.3. Since the agreement of values is so strong, it can be concluded that the result proved analytically has been demonstrated through numerical computation.

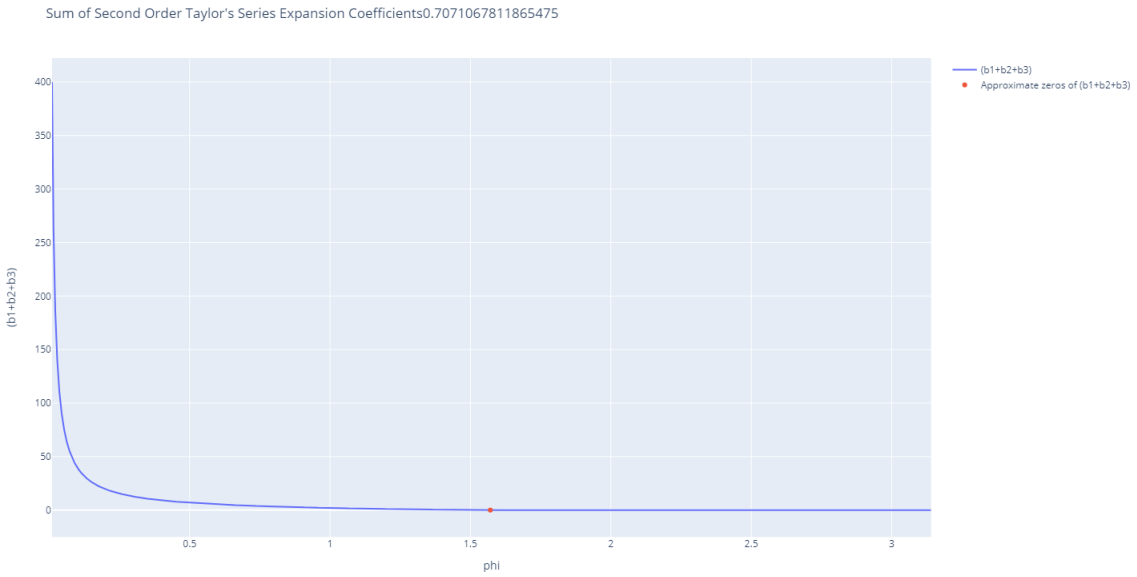

Figure 6.3: Second Order Taylor's Series Expansion Coefficients at $r = \frac{1}{\sqrt{2}}$

7. FUTURE WORK

The present work may be thought of as a specific instance of planning the motion of a rigid stick on a sphere with a geodesic curvature constraint. The motion planning problem of a UAV (modeled as a stick) will require a generalization of this work, especially when the initial and final configurations of the stick lie on different spheres.

REFERENCES

[1] L. E. Dubins, "On curves of minimal length with a constraint on average curvature, and with prescribed initial and terminal positions and tangents," *American Journal of Mathematics*, vol. 79, no. 3, pp. 497–516, 1957.

[2] F. Monroy-Pérez, "Non-euclidean dubins' problem.," *Journal of Dynamical and Control Systems*, vol. 4, no. 2, p. 249, 1998.

[3] J. REEDS and L. SHEPP, "Optimal paths for a car that goes both forwards and backwards.," *PACIFIC JOURNAL OF MATHEMATICS*, vol. 145, no. 2, pp. 367 – 393, 1990.

[4] J.-D. Boissonnat, A. Cerezo, and J. Leblond, "Shortest paths of bounded curvature in the plane.," *Proceedings 1992 IEEE International Conference on Robotics and Automation, Robotics and Automation, 1992. Proceedings., 1992 IEEE International Conference on*, p. 2315, 1992.

[5] V. A. Toponogov, *Differential geometry of curves and surfaces*. Springer, 2006.

[6] J. Ayala, D. Kirszenblat, and J. H. Rubinstein, "A geometric approach to shortest bounded curvature paths," 2015.

[7] S. G. Manyam, S. Rathinam, D. Casbeer, and E. Garcia, "Tightly bounding the shortest dubins paths through a sequence of points," *Journal of Intelligent & Robotic Systems*, vol. 88, no. 2, pp. 495–511, 2017.

[8] S. G. Manyam and S. Rathinam, "On tightly bounding the dubins traveling salesman's optimum," *Journal of Dynamic Systems, Measurement, and Control*, vol. 140, no. 7, 2018.

[9] J. Baek, A. Deopurkar, and K. Redfield, "Finding geodesics on surfaces," *Dept. Comput. Sci., Stanford Univ., Stanford, CA, USA, Tech. Rep*, 2007.

[10] H. J. Sussmann and J. C. Willems, "300 years of optimal control: from the brachystochrone to the maximum principle," *IEEE Control Systems Magazine*, vol. 17, no. 3, pp. 32–44, 1997.

APPENDIX A

INTERMEDIATE CALCULATIONS

Symbols used

$$\Omega_L = \begin{pmatrix} 0 & -r & 0 \\ r & 0 & -\sqrt{1-r^2} \\ 0 & \sqrt{1-r^2} & 0 \end{pmatrix} \qquad \Omega_R = \begin{pmatrix} 0 & -r & 0 \\ r & 0 & \sqrt{1-r^2} \\ 0 & -\sqrt{1-r^2} & 0 \end{pmatrix}$$

$$\Omega_L^2 = \begin{pmatrix} -r^2 & 0 & r\sqrt{1-r^2} \\ 0 & -1 & 0 \\ r\sqrt{1-r^2} & 0 & -(1-r^2) \end{pmatrix} \quad \Omega_R^2 = \begin{pmatrix} -r^2 & 0 & -r\sqrt{1-r^2} \\ 0 & -1 & 0 \\ -r\sqrt{1-r^2} & 0 & -(1-r^2) \end{pmatrix}$$

$$\mathbf{u}_L = \begin{pmatrix} \sqrt{1-r^2} \\ 0 \\ r \end{pmatrix} \qquad \mathbf{u}_R = \begin{pmatrix} -\sqrt{1-r^2} \\ 0 \\ r \end{pmatrix}$$

$$R_L(\pi+\theta) = I - \Omega_L \sin\theta + \Omega_L^2(1+\cos\theta)$$

$$R_R(\pi+\theta) = I - \Omega_R \sin\theta + \Omega_R^2(1+\cos\theta)$$

$$e_2^* = \begin{pmatrix} 0 & 1 & 0 \end{pmatrix} \qquad e_2 = \begin{pmatrix} 0 \\ 1 \\ 0 \end{pmatrix}$$

Repeatedly used Calculations

$$\Omega_L \mathbf{u}_R = -2r\sqrt{1-r^2}e_2 \qquad \Omega_R \mathbf{u}_L = 2r\sqrt{1-r^2}e_2$$

$$\mathbf{u}_L^*\Omega_R^2 = -2r\sqrt{1-r^2}\begin{pmatrix} r & 0 & \sqrt{1-r^2}\end{pmatrix}$$
$$\mathbf{u}_R^*\Omega_L^2 = -2r\sqrt{1-r^2}\begin{pmatrix} -r & 0 & \sqrt{1-r^2}\end{pmatrix}$$

$$\Omega_R^2\mathbf{u}_L = -2r\sqrt{1-r^2}\begin{pmatrix} r \\ 0 \\ \sqrt{1-r^2}\end{pmatrix} \qquad \Omega_L^2\mathbf{u}_R = -2r\sqrt{1-r^2}\begin{pmatrix} -r \\ 0 \\ \sqrt{1-r^2}\end{pmatrix}$$

$$\Omega_L\mathbf{u}_L = \Omega_R\mathbf{u}_R = \mathbf{u}_L^*\Omega_L = \mathbf{u}_R^*\Omega_R = 0$$

$$\mathbf{u}_R^*R_R(\pi+\phi) = \mathbf{u}_R^* \qquad \mathbf{u}_L^*R_L(\pi+\phi) = \mathbf{u}_L^*$$
$$R_R(\pi+\phi)\mathbf{u}_R = \mathbf{u}_R \qquad R_L(\pi+\phi)\mathbf{u}_L = \mathbf{u}_L$$

Solutions to previously mentioned equations

Equation 4.28 is

$$0 = a_1\mathbf{u}_L^*\Omega_R R_R(\pi+\phi)R_L(\pi+\phi)\mathbf{u}_R + a_2\mathbf{u}_L^*R_R(\pi+\phi)R_L(\pi+\phi)\Omega_L\mathbf{u}_R \tag{A.1}$$

In equation A.1 above, the coefficient of a_1 is evaluated using the previously mentioned repeated calculations to give:

$$\mathbf{u}_L^*\Omega_R R_R(\pi+\phi)R_L(\pi+\phi)\mathbf{u}_R = (2r\sqrt{1-r^2})^2[\sin\phi\cos\phi - (1-2r^2)\sin\phi(1+\cos\phi]$$

Similarly, the coefficient of a_2 is determined to be:

$$\mathbf{u}_L^*R_R(\pi+\phi)R_L(\pi+\phi)\Omega_L\mathbf{u}_R = (2r\sqrt{1-r^2})^2[\sin\phi\cos\phi - (1-2r^2)\sin\phi(1+\cos\phi]$$

Therefore, equation A.1 after substitution, gives:

$$a_1 = -a_2 \tag{A.2}$$

Equation 4.29 is

$$\mathbf{u}_R^* \Omega_L R_R(\pi + \phi)\mathbf{u}_L = a_3 \mathbf{u}_R^* R_L(\pi + \phi)\Omega_R \mathbf{u}_L \tag{A.3}$$

L.H.S of equation A.3 gives:

$$\mathbf{u}_R^* \Omega_L R_R(\pi + \phi)\mathbf{u}_L = -(2r\sqrt{1 - r^2})^2 \sin\phi$$

Coefficient of a_3 in A.3 gives:

$$\mathbf{u}_R^* R_L(\pi + \phi)\Omega_R \mathbf{u}_L = -(2r\sqrt{1 - r^2})^2 \sin\phi$$

Therefore, equation A.3 upon solving gives:

$$a_3 = 1 \tag{A.4}$$

Equation 4.30 upon performing mentioned operation gives:

$$\mathbf{u}_R^* \Omega_L R_R(\pi + \phi) R_L(\pi + \phi)\mathbf{u}_R = a_2 \mathbf{u}_R^* R_L(\pi + \phi)\Omega_L \mathbf{u}_R \tag{A.5}$$

L.H.S of equation A.5 gives:

$$\mathbf{u}_R^* \Omega_L R_R(\pi + \phi) R_L(\pi + \phi)\mathbf{u}_R = (2r\sqrt{1 - r^2})^2 \sin\phi((1 - 2r^2)(1 + \cos\phi) - \cos\phi)$$

Coefficient of a_2 in equation A.5 gives:

$$\mathbf{u}_R^* R_L(\pi + \phi)\Omega_L \mathbf{u}_R = (2r\sqrt{1 - r^2})^2 \sin\phi$$

Thus, equation A.5 solved gives:

$$a_2 = -[\cos\phi - (1-2r^2)(1+\cos\phi)]$$

Thus, a_1, a_2, and a_3 are determined to be:

$$a_1 = \cos\phi - (1-2r^2)(1+\cos\phi); \quad a_2 = -[\cos\phi - (1-2r^2)(1+\cos\phi)];$$
$$a_3 = 1$$

Equation 4.34 upon performing the mentioned operation gives:

$$\begin{aligned} 0 &= b_1[\mathbf{u}_L^*\Omega_R R_R(\pi+\phi)R_L(\pi+\phi)\mathbf{u}_R] + a_1^2[\mathbf{u}_L^*\Omega_R^2 R_R(\pi+\phi)R_L(\pi+\phi)\mathbf{u}_R] \\ &+ 2a_1a_2[\mathbf{u}_L^*\Omega_R R_R(\pi+\phi)R_L(\pi+\phi)\Omega_L\mathbf{u}_R] + b_2[\mathbf{u}_L^* R_R(\pi+\phi)R_L(\pi+\phi)\Omega_L\mathbf{u}_R] \\ &+ a_2^2[\mathbf{u}_L^* R_R(\pi+\phi)R_L(\pi+\phi)\Omega_L^2\mathbf{u}_R] \end{aligned} \tag{A.6}$$

The coefficient of b_1 in equation A.6 is determined to be:

$$\begin{aligned} &\mathbf{u}_L^*\Omega_R R_R(\pi+\phi)R_L(\pi+\phi)\mathbf{u}_R \\ &= (2r\sqrt{1-r^2})^2(\sin\phi)(\cos\phi - (1-2r^2)(1+\cos\phi)) \\ &= (2r\sqrt{1-r^2})^2(\sin\phi)a_1 \end{aligned}$$

Similarly, the coefficients of a_1^2, $2a_1a_2$, b_2, and a_2^2 are determined to be:

$$\begin{aligned}
&\mathbf{u}_L^*\Omega_R^2 R_R(\pi+\phi)R_L(\pi+\phi)\mathbf{u}_R \\
&= -(2r\sqrt{1-r^2})^2(1-\cos^2\phi+(1-2r^2)\cos\phi(1+\cos\phi)) \\
&\mathbf{u}_L^*\Omega_R R_R(\pi+\phi)R_L(\pi+\phi)\Omega_L\mathbf{u}_R \\
&= (2r\sqrt{1-r^2})^2((1-2r^2)(1-\cos^2\phi)+\cos^2\phi) \\
&\mathbf{u}_L^* R_R(\pi+\phi)R_L(\pi+\phi)\Omega_L\mathbf{u}_R \\
&= \mathbf{u}_L^*\Omega_R R_R(\pi+\phi)R_L(\pi+\phi)\mathbf{u}_R \\
&= (2r\sqrt{1-r^2})^2(\sin\phi)(\cos\phi-(1-2r^2)(1+\cos\phi)) \\
&= (2r\sqrt{1-r^2})^2(\sin\phi)a_1 \\
&\mathbf{u}_L^* R_R(\pi+\phi)R_L(\pi+\phi)\Omega_L^2\mathbf{u}_R \\
&= \mathbf{u}_L^*\Omega_R^2 R_R(\pi+\phi)R_L(\pi+\phi)\mathbf{u}_R \\
&= -(2r\sqrt{1-r^2})^2(1-\cos^2\phi+(1-2r^2)\cos\phi(1+\cos\phi))
\end{aligned}$$

Thus, equation A.6 simplifies upon substituting the above determined expressions to:

$$(b_1+b_2)\sin\phi = 4\cos^2\phi(-2r^4+r^2)+2\cos\phi(-8r^4+8r^2-1)-8r^4+12r^2-4 \tag{A.7}$$

Equation 4.35 upon performing the mentioned operation gives:

$$\begin{aligned}
\mathbf{u}_R^*\Omega_L^2 R_R(\pi+\phi)R_L(\pi+\phi)\mathbf{u}_L = 2a_2a_3[\mathbf{u}_R^* R_R(\pi+\phi)R_L(\pi+\phi)\Omega_L\Omega_R\mathbf{u}_L] \\
+ b_3[\mathbf{u}_R^* R_R(\pi+\phi)R_L(\pi+\phi)\Omega_R\mathbf{u}_L] + a_3^2[\mathbf{u}_R^* R_R(\pi+\phi)R_L(\pi+\phi)\Omega_R^2\mathbf{u}_L]
\end{aligned} \tag{A.8}$$

The L.H.S of A.8 is determined to be:

$$\mathbf{u}_R^*\Omega_L^2 R_R(\pi+\phi)R_L(\pi+\phi)\mathbf{u}_L = (2r\sqrt{1-r^2})^2(1-2r^2)(1+\cos\phi)$$

The coefficients of $2a_2a_3$, b_3, and a_3^2 respectively are:

$$\mathbf{u}_R^* R_R(\pi+\phi)R_L(\pi+\phi)\Omega_L\Omega_R\mathbf{u}_L = -(2r\sqrt{1-r^2})^2\cos\phi$$
$$\mathbf{u}_R^* R_R(\pi+\phi)R_L(\pi+\phi)\Omega_R\mathbf{u}_L = -(2r\sqrt{1-r^2})^2\sin\phi$$

$$\begin{aligned}\mathbf{u}_R^* R_R(\pi+\phi)R_L(\pi+\phi)\Omega_R^2\mathbf{u}_L &= \mathbf{u}_R^*\Omega_L^2 R_R(\pi+\phi)R_L(\pi+\phi)\mathbf{u}_L \\ &= (2r\sqrt{1-r^2})^2(1-2r^2)(1+\cos\phi)\end{aligned}$$

Substituting the coefficients determined above into equation A.8 gives:

$$b_3\sin\phi = 4\cos^2\phi r^2 + 2\cos\phi(2r^2-1) \tag{A.9}$$

Equation 4.36 upon performing the mentioned operation gives:

$$\begin{aligned}\mathbf{u}_R^*\Omega_L^2 R_R(\pi+\phi)R_L(\pi+\phi)\mathbf{u}_R &= b_2[\mathbf{u}_R^* R_R(\pi+\phi)R_L(\pi+\phi)\Omega_L\mathbf{u}_R] \\ &\quad + a_2^2[\mathbf{u}_R^* R_R(\pi+\phi)R_L(\pi+\phi)\Omega_L^2\mathbf{u}_R]\end{aligned} \tag{A.10}$$

The L.H.S of A.10 gives:

$$\begin{aligned}&\mathbf{u}_R^*\Omega_L^2 R_R(\pi+\phi)R_L(\pi+\phi)\mathbf{u}_R \\ &= (2r\sqrt{1-r^2})^2(\cos\phi - (1-2r^2)(1-\cos^2\phi) - (1-2r^2)^2(1+\cos\phi)^2\end{aligned}$$

The coefficients of b_2, and a_2^2 are:

$$\mathbf{u}_R^* R_R(\pi+\phi)R_L(\pi+\phi)\Omega_L\mathbf{u}_R = (2r\sqrt{1-r^2})^2\sin\phi$$
$$\mathbf{u}_R^* R_R(\pi+\phi)R_L(\pi+\phi)\Omega_L^2\mathbf{u}_R = (2r\sqrt{1-r^2})^2\cos\phi$$

Upon substituting the above determined expressions and solving, equation A.10 gives:

$$b_2\sin\phi = -4\cos^3 r^4 + \cos^2\phi(-12r^4+6r^2) + \cos\phi(-12r^4+12r^2-2) - 4r^4 + 6r^2 - 2 \tag{A.11}$$

Thus, equations A.7, A.9, and A.11 give the following solution:

$$b_1 \sin\phi = 4\cos^3\phi r^4 + \cos^2\phi(4r^4 - 2r^2) + \cos\phi(-4r^4 + 4r^2) - 4r^4 + 6r^2 - 2$$

$$b_2 \sin\phi = -4\cos^3\phi r^4 + \cos^2\phi(-12r^4 + 6r^2) + \cos\phi(-12r^4 + 12r^2 - 2)$$
$$- 4r^4 + 6r^2 - 2$$

$$b_3 \sin\phi = 4\cos^2\phi r^2 + \cos\phi(4r^2 - 2)$$

Thus, equation 4.37 is arrived at:

$$(b_1 + b_2 + b_3)\sin\phi = \cos^2\phi(-8r^4 + 8r^2) + \cos\phi(-16r^4 + 20r^2 - 4) - 8r^4 + 12r^2 - 4$$

Denote for compactness:

$$\lambda = r^2, \qquad P = \cos\phi, \qquad R = \sin\phi$$

Using this notation, 4.38 is written using the following equation:

$$(b_1 + b_2 + b_3)R = P^2(-8\lambda^2 + 8\lambda) + P(-16\lambda^2 + 20\lambda - 4) - 8\lambda^2 + 12\lambda - 4 < 0 \qquad \text{(A.12)}$$

Simplification of the inequality on the R.H.S of equation A.12 above is as follows:

$$P^2(-8\lambda^2 + 8\lambda) + P(-16\lambda^2 + 20\lambda - 4) - 8\lambda^2 + 12\lambda - 4 < 0$$

$$2P^2(-\lambda^2 + \lambda) + P(-4\lambda^2 + 5\lambda - 1) - 2\lambda^2 + 3\lambda - 1 < 0$$

$$2P^2(\lambda^2 - \lambda) - P(-4\lambda^2 + 5\lambda - 1) + 2\lambda^2 - 3\lambda + 1 > 0$$

$$\lambda^2(2P^2 + 4P + 2) - \lambda(2P^2 + 5P + 3) + (P + 1) > 0$$

$$2\lambda^2(P + 1)^2 - \lambda(2P + 3)(P + 1) + (P + 1) > 0$$

$$2\lambda^2(P + 1) - \lambda(2P + 3) + 1 > 0$$

Thus, the compact version of the inequality to prove, inequality 4.39 is arrived at.

APPENDIX B

MATHEMATICAL BASIS FOR THE COMPUTATION

Given initial position u, initial velocity U, final position v, final velocity V, turning radius constraint r, and sphere radius R, the main set of codes returns the list of all potential optimal paths that can be taken from the initial configuration to the final configuration. Note that a configuration consists of both position and velocity.

From the theorems discussed in the main section of this report, it is theorized that potential optimal paths can be of the following types:

1. CGC
2. CCC
3. CG
4. GC
5. CC
6. C

The steps involved in computing the potential optimal paths are as Based on the types of paths that could potentially be optimal, we have the following formulae for path lengths based on the arc length formula:

1. $L_{CGC} = (\xi + \beta)r + \eta R$
2. $L_{CCC} = (\xi + \beta)r + \eta R$
3. $L_{CG} = \xi r + \beta R$
4. $L_{GC} = \beta R + \xi r$

5. $L_{CC} = (\xi + \eta)r$

6. $L_C = \xi r$

Where in the above, ξ, β, η represent angles of turn corresponding to the initial, tangent, and final circular arcs of the path in question. Note that the tangent circular arc can be either a great circular arc or a small circular arc based on the minimum turning radius constraint. follows:

1. Find initial and final tight circle centers.

2. Determine what types of paths are possible

3. Find tangent circle to both initial and final tight circles (can be a great circle in the case of CGC, GC or CG; or a tight circle in case of CCC).

4. Find tangent points.

5. Find velocities at tangent points in order to determine angles.

6. Find path length L using angles determined in the previous step.

B.1 Find initial and final tight circle centers

Required conditions for the 2 initial tight circle centers (represented as dU are as follows:

$$\begin{aligned} (u - dU) \cdot dU &= 0 \\ (u - dU) \cdot U &= 0 \end{aligned} \tag{B.1}$$

Equations B.1 imply that $u - dU$ is in the plane of $U \times dU$. Using this fact we have:

$$\begin{aligned} \|u - dU\| &= \mid \alpha \mid \|U \times dU\| \\ \alpha &= \pm \frac{r}{\sqrt{(U \cdot U)(dU) \cdot (dU) - (U \cdot dU)^2}} \end{aligned} \tag{B.2}$$

Thus, the equation required to find dU is:

$$u = (I + \alpha[U]_\times)dU \tag{B.3}$$

In the above, $[U]_\times$ is the unique skew-symmetric matrix associated with the vector U and I is the identity matrix. dU can thus be found using u, U, r which are given. Similarly dV which represent the centers of circles associated with the final configuration are determined using v, V, r. Note that there are 2 tight circles associated with the initial configuration and 2 associated with the final configuration.

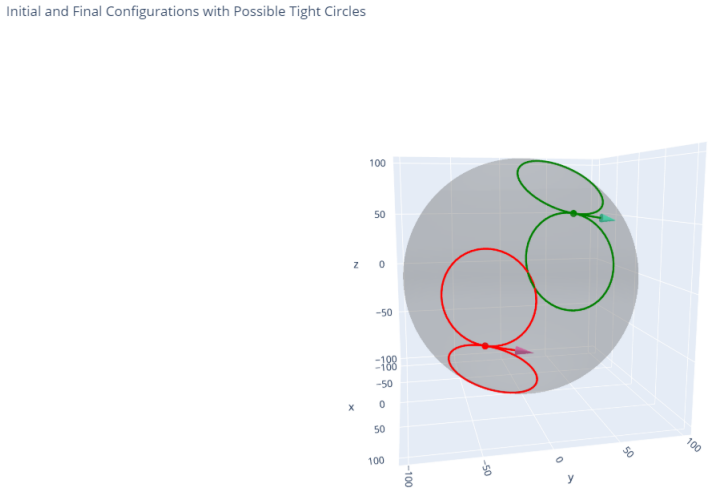

Figure B.1: Possible Tight Circles Determined

B.2 Find Tangent Circle to the Tight Circles associated with the Configurations

Before getting to the method of determining the centers of the tangent circles to the tight circles associated with the initial and final configurations, it must be noted that, pairs of tight circles must be considered with one from the initial configuration and one from the final configuration. For each of these pairs, the check must be done to figure out which kinds of tangent circles are possible

resulting in CGC or a degenerate case containing a G, CCC, CC, or C path. In the pair of tight circles considered, let the initial tight circle be represented by c_u and the final one be represent by c_v. The checks are as follows:

B.2.1 C Type Path

$$c_u = c_v \tag{B.4}$$

B.2.2 CC Type Path

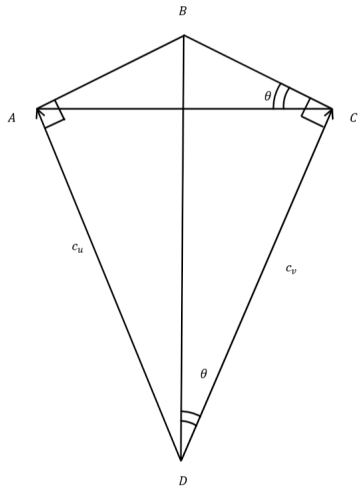

Figure B.2: Limit for CC Case

In the figure B.2, D is the origin, $EB = y$, $EC = x$, $BC = r$, $DC = AD = R1 = \sqrt{R^2 - r^2}$. Notice that in the figure, the lines AB, and BC represent the parts of 2 tight circles touching each other at point B. Refer to the figure above to notice the following facts.

$$\begin{aligned} &\tan\theta = \frac{y}{x} = \frac{x}{R-y} \implies x^2 = y(R-y); \\ &x^2 + y^2 = r^2 \end{aligned} \tag{B.5}$$

From the equations B.5, we have the following condition for CC type paths:

$$\|c_u - c_v\| = 2x = 2\sqrt{r^2 - \frac{r^4}{R^2}} \tag{B.6}$$

B.2.3 CCC Type Path

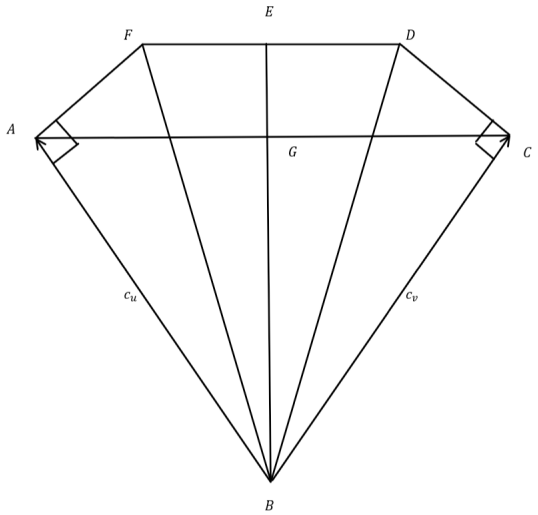

Figure B.3: Limit for CCC Case

In the figure B.3, B is the origin, $BC = AB = R1 = \sqrt{R^2 - r^2}$, $BD = BF = R$, and $DC = ED = EF = FA = r$. Notice the following facts:

$$\begin{aligned}
&Area_{AFEDCB} = 4(Area_{BCD}) = 4(\frac{1}{2})r(R1) = 2rR1 \\
&Area_{AFEDCG} = \frac{1}{2}(2r + AC)(EG) = 2r(R1) - \frac{1}{2}(AC)(BG) \\
&BG = R1\cos(2\theta) = R1(2\cos^2(\theta)) - 1 \\
&EG = R1 - R1\cos(2\theta) \\
&\cos(2\theta) = 2\left(\frac{R1}{R}\right)^2 - 1 \\
&AC = \frac{4rR1 - 2r(EG)}{EG + BG} = 4r\left(1 + \frac{4rR1^2}{R^2}\right)
\end{aligned} \tag{B.7}$$

Thus, the condition for CCC case is:

$$\|c_u - c_v\| \leq 4r\left(1 + \frac{4rR1^2}{R^2}\right) \tag{B.8}$$

B.3 CGC Type Paths

For CGC type paths, there are 2 possibilities, the CGC path can be on a direct tangent plane or a cross tangent place to the pair of tight circles. The direct tangent plane is one that is tangent to the tight circles and is on the same side of the circles. The cross tangent plane is one that is tangent to the 2 circles and is on either side of them. This can be understood by the illustrations B.4 and B.5. In the codes, the CGC, GC, CG, G type paths are all handled by a single module.

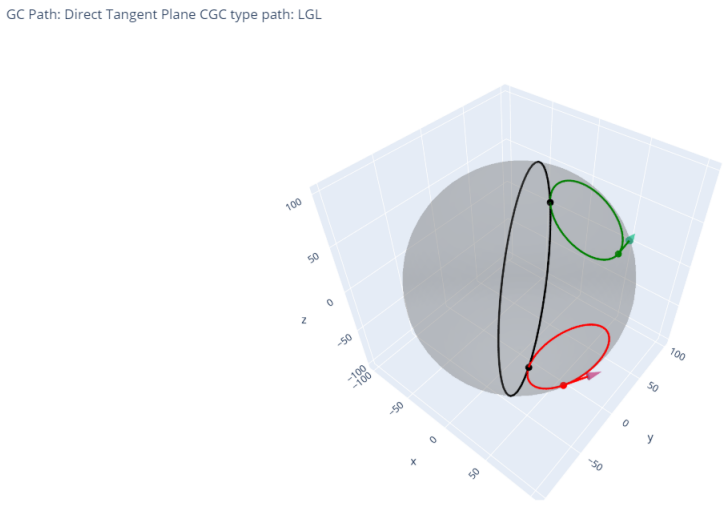

Figure B.4: Direct Tangent Plane

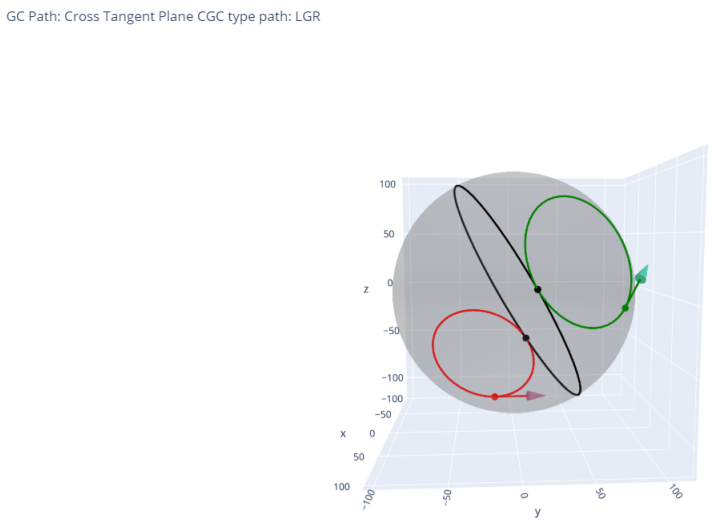

Figure B.5: Cross Tangent Plane

B.4 Finding the Tangent Circles

B.4.1 Finding the Great Circle Plane

Denote the great circle planes by w (notice how multiple planes are denoted by just one symbol).

B.4.1.1 Direct Tangent Plane

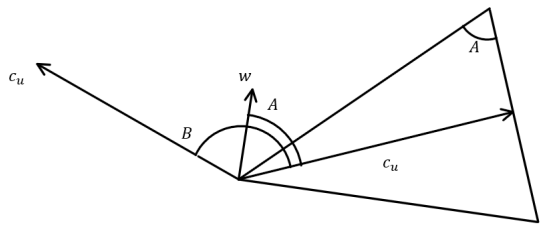

Figure B.6: Unit Normal to Great Circle Plane

The figure B.6 will aid in understanding the equations that follow.

$$\begin{aligned} w \cdot c_u &= \cos A \\ w \cdot c_v &= \cos A \\ \text{Define } B &= \arccos(c_u \cdot c_v) \end{aligned} \tag{B.9}$$

Notice that the c_u, c_v vectors have been normalized. From the above, we have:

$$w \cdot (c_u - c_v) = 0; \tag{B.10}$$

and since $(c_u - c_v) \cdot (c_u + c_v) = 0$, we have that $(c_u - c_v)$, $(c_u + c_v)$, and $(c_u \times c_v)$ form an orthogonal triplet; and therefore that:

$$w = \phi\left(\frac{c_u + c_v}{\|c_u + c_v\|}\right) + \psi\left(\frac{c_u \times c_v}{\|c_u \times c_v\|}\right) \tag{B.11}$$

Using this setup and determining ϕ and ψ values to be such that the w determined is of unit magnitude, the following are the necessary equations for determining w:

$$\begin{aligned} \phi &= \frac{2\cos(A)}{\sqrt{2 + 2\cos(B)}} \\ \psi &= \pm\sqrt{1 - \frac{1 + \cos(2A)}{1 + \cos(B)}} \end{aligned} \tag{B.12}$$

and since $\|w\| = 1$, the condition to be satisfied for the plane to be a direct tangent plane:

$$\cos(2A) \leq cos(B) \tag{B.13}$$

B.4.1.2 Cross Tangent Plane

The figure B.6 will aid in understanding the equations that follow.

$$\begin{aligned} w \cdot c_u &= \cos A \\ (-w) \cdot c_v &= \cos A \\ \text{Define } B &= \arccos(c_u \cdot c_v) \end{aligned} \tag{B.14}$$

Notice that the c_u, c_v vectors have been normalized. From the above, we have:

$$w \cdot (c_u + c_v) = 0; \tag{B.15}$$

and since $(c_u - c_v) \cdot (c_u + c_v) = 0$, we have that $(c_u - c_v)$, $(c_u + c_v)$, and $(c_u \times c_v)$ form an orthogonal triplet; and therefore that:

$$w = \phi\left(\frac{c_u - c_v}{\|c_u - c_v\|}\right) + \psi\left(\frac{c_u \times c_v}{\|c_u \times c_v\|}\right) \tag{B.16}$$

Using this setup and determining ϕ and ψ values to be such that the w determined is of unit magnitude, the following are the necessary equations for determining w:

$$\begin{aligned} \phi &= \frac{2\cos(A)}{\sqrt{2 - 2\cos(B)}} \\ \psi &= \pm\sqrt{1 - \frac{1 + \cos(2A)}{1 + \cos(B)}} \end{aligned} \tag{B.17}$$

and since $\|w\| = 1$, the condition to be satisfied for the plane to be a direct tangent plane:

$$\cos(2A) + \cos(B) \leq 0 \tag{B.18}$$

B.5 Finding the Tangent Tight Circle Centers

Denote the tangent tight circles between a pair of initial and final tight circles to be c_t. Since the angle between the tangent tight circle center vector and each of the initial and final tight circle centers, we have:

$$\begin{aligned} &c_u \cdot c_t = \cos(\bar{A}) \\ &c_v \cdot c_t = \cos(\bar{A}) \\ &\text{Define } \bar{A} = \arctan\left(\frac{r}{R1}\right) = \arctan\left(\frac{r}{\sqrt{R^2 - r^2}}\right) \end{aligned} \tag{B.19}$$

In a similar manner as before, we get the following equations that determine c_t:

$$\begin{aligned} \phi &= \frac{2\cos(\bar{A})}{\sqrt{2 + 2\cos(B)}} \\ \psi &= \pm\sqrt{1 - \frac{1 + \cos(2\bar{A})}{1 + \cos(B)}} \\ c_t &= \phi\left(\frac{c_u + c_v}{\|c_u + c_v\|}\right) + \psi\left(\frac{c_u \times c_v}{\|c_u \times c_v\|}\right) \end{aligned} \tag{B.20}$$

B.6 Finding the Tangent Points

B.6.1 CGC Case

B.6.1.1 Direct Tangent Plane

The figure B.7 will aid in understanding the equations that follow. In what follows, T is a vector in the same direction as the tangent point, c is the center of the tight circle and w is the unit normal to the great circle plane (the pair for which the tangent point is to be determined), $\hat{t}$ is T

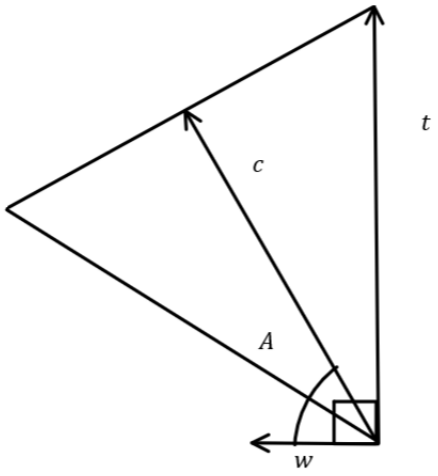

Figure B.7: Cross Tangent Plane case when $\cos$ A>0

normalized and t is the tangent point itself.

$$
\begin{aligned}
T &= c - \frac{< c, w >}{< w, w >} w = c - \sqrt{R^2 - r^2}\left(\frac{r}{R}\right) w \\
\hat{t} &= \frac{T}{\|T\|} \\
t &= R\hat{t}
\end{aligned}
\tag{B.21}
$$

B.6.1.2 Cross Tangent Plane

The figures B.8 and B.9 will aid in understanding the equations that follow. In what follows, T is a vector in the same direction as the tangent point, c is the center of the tight circle and w is the unit normal to the great circle plane (the pair for which the tangent point is to be determined), $\hat{t}$ is T normalized and t is the tangent point itself.

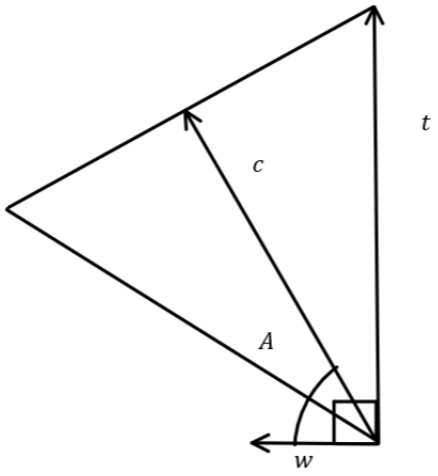

Figure B.8: Cross Tangent Plane case when $\cos$ A>0

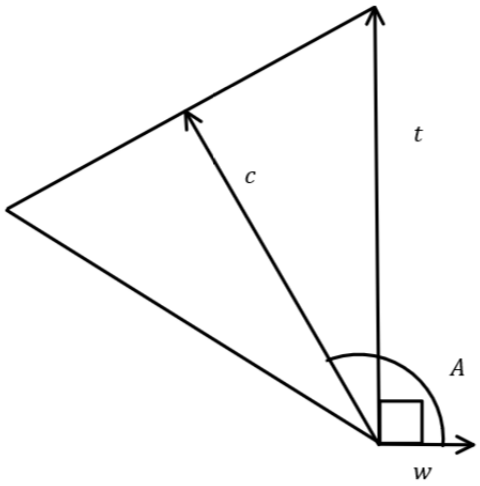

Figure B.9: Cross Tangent Plane case when $\cos$ A<0

If $\cos A > 0$, then the following holds:

$$
\begin{aligned}
T &= c - \frac{< c, w >}{< w, w >} w = c - \sqrt{R^2 - r^2}\left(\frac{r}{R}\right) w \\
\hat{t} &= \frac{T}{\|T\|} \\
t &= R\hat{t}
\end{aligned}
\tag{B.22}
$$

if $\cos A < 0$, then the following holds:

$$\begin{aligned} T &= c - \frac{< c, w >}{< w, w >}(-w) = c + \sqrt{R^2 - r^2}\left(\frac{r}{R}\right)w \\ \hat{t} &= \frac{T}{\|T\|} \\ t &= R\hat{t} \end{aligned} \tag{B.23}$$

B.6.2 CCC case

In what follows, c_u represents the initial tight circle in question, c_v represents the final tight circle in question, and c_t represents the tangent tight circle connecting the two.

$$\begin{aligned} T &= c_u + \frac{(c_t - c_u)}{2} \\ \hat{t} &= \frac{T}{\|T\|} \\ t &= R\hat{t} \end{aligned} \tag{B.24}$$

In a very similar way, the tangent point is of CC type.

B.7 Tangent Vectors (or Velocity) at the Tangent Points

To determine the tangent vectors determinants are used since they are used to find the orientation of 3 vectors with respect to each other. c represents the center of the circle on which a tangent is to be found, p represents the position at which a tangent is to be constructed and vel represents a known velocity like U or V initially. Denote:

$$c = \begin{pmatrix} c_1 \\ c_2 \\ c_3 \end{pmatrix}; \quad p = \begin{pmatrix} p_1 \\ p_2 \\ p_3 \end{pmatrix}; \quad vel = \begin{pmatrix} vel_1 \\ vel_2 \\ vel_3 \end{pmatrix}; \quad D = det \begin{pmatrix} c_1 & c_2 & c_3 \\ p_1 - c_1 & p_2 - c_2 & p_3 - c_3 \\ vel_1 & vel_2 & vel_3 \end{pmatrix} \tag{B.25}$$

If $D > 0$, then the known tangent vector represents a left turn about the arc of the circle c.

If $D < 0$, then the known tangent vector represents a right turn about the arc of the circle c.

Figure B.10 illustrates a right turn about the circle. Note that c and p in the diagram and coming out of the plane. The relationship between a determinant and the 3 row vectors it is made up of can be used in conjunction with the right hand screw rule to verify the equations above.

To find the required tangent vector (represented by t), the sense of rotation about the circle on

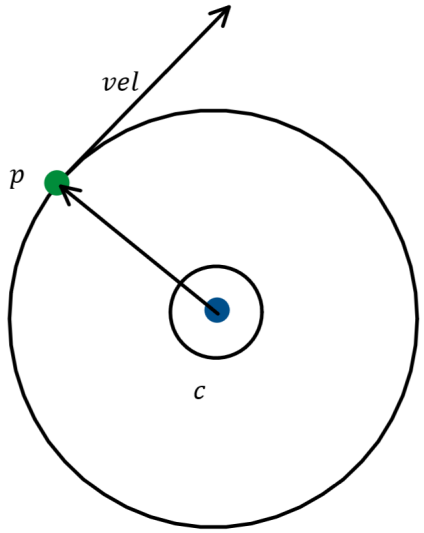

Figure B.10: Right Turn: D<0

which it needs to be constructed must be known. This is determined by D above. Now, using D:

If $D < 0$, then: $t = -(c \times (t - c))$

If $D > 0$, then: $t = c \times (t - c)$

B.8 Finding the Angles

In what follows c is the center of the circle of which the arc is a part, p_1 and p_2 are the initial and final positions on the circle describing the arc in question, and t is the velocity at p_1. The angle

to be found is the angle of the arc just described. Denote:

$$c = \begin{pmatrix} c_1 \\ c_2 \\ c_3 \end{pmatrix}; \quad p_1 = \begin{pmatrix} p_{11} \\ p_{12} \\ p_{13} \end{pmatrix}; \quad p_2 = \begin{pmatrix} p_{21} \\ p_{22} \\ p_{23} \end{pmatrix}; \quad t = \begin{pmatrix} t_1 \\ t_2 \\ t_3 \end{pmatrix}; \tag{B.26}$$

We then have the following:

$$D_1 = det \begin{pmatrix} c_1 & c_2 & c_3 \\ p_{11} - c_1 & p_{12} - c_2 & p_{13} - c_3 \\ t_1 & t_2 & t_3 \end{pmatrix} \quad D_2 = det \begin{pmatrix} p_{11} - c_1 & p_{12} - c_2 & p_{13} - c_3 \\ p_{21} - c_1 & p_{22} - c_2 & p_{23} - c_3 \\ c_1 & c_2 & c_3 \end{pmatrix} \tag{B.27}$$

Using the above determinants, we have the following:

If $D_1 D_2 > 0$, then the angle between p_1 and p_2 represented by θ is as follows:

$$\theta = \arccos\left(\frac{< p_1 - c, p_2 - c >}{\|p_1 - c\| \|p_2 - c\|}\right) \tag{B.28}$$

However, if $D_1 D_2 < 0$ then we have:

$$\theta = 2\pi - \arccos\left(\frac{< p_1 - c, p_2 - c >}{\|p_1 - c\| \|p_2 - c\|}\right) \tag{B.29}$$

The 2 cases above have been illustrated in figures B.11 and B.12 and they can be verified using the right hand screw rule.

The above method can be used appropriately to find all required angles by constructing tangent vectors wherever required.

B.9 Finding Path Length

Note that ξ and β represent angles about initial and final tight circle centers respectively, and η represents angles about tangent circle centers (may be tangent tight circle or great circle). We then

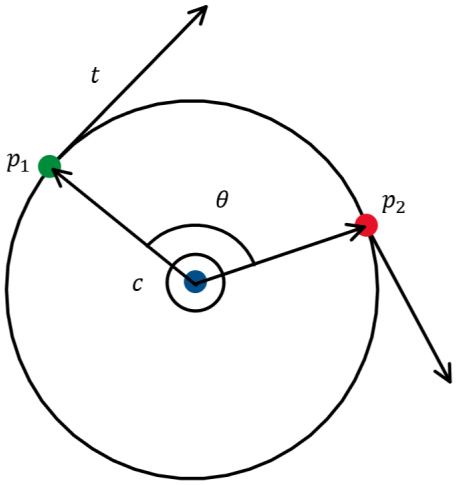

Figure B.11: Angle when D1D2>0

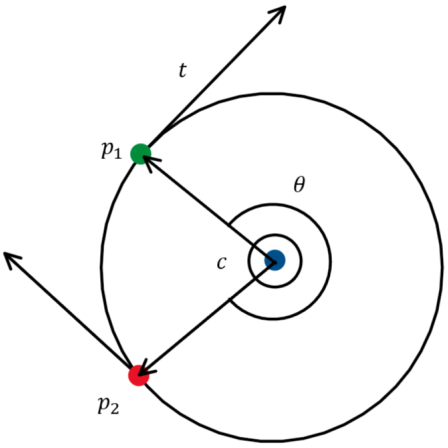

Figure B.12: Angle when D1D2<0

have the following:

$$L_{CGC} = (\xi + \beta)r + \eta R$$

$$L_{CCC} = (\xi + \eta + \beta)r$$

$$L_{CG} = \xi r + \eta R$$

$$L_{GC} = \eta R + \beta r$$

$$L_{CC} = (\eta + \beta)r$$

$$L_C = \xi r$$

Thus, all required geometrical data has been determined using only what is given as input to the main set of codes (in which these calculations are performed). Recall that the input variables are u, U, v, V, r, R.

The only other concept used in the computation is the Euler-Rodrigues' rotation formula which is used in the second code for construction of the path whose length is to be compared with all potential optimal path.

APPENDIX C

CODES AND DATA SETS

C.1 Main Set of Codes

The codes used to determine all optimal paths given initial and final configurations, minimum turning radius constraint r, and sphere radius R are as follows:

- *IconfigFconfig.py*: The main module of this set of codes which calls functions from all other modules.
- *SphereGenerate.py*: The module that generates all required geometrical constructions.
- *SphereDetermine.py*: The next module is the one that determines all important geometrical data discussed in the previous appendix.
- *GCPaths.py*: The module that handles all Dubins' types paths containing a G segment (CGC, GC, CG, G) calling *SphereGenerate.py* and *SphereDetermine.py* as required.
- *threeTCPaths.py*: The module that handles CCC paths calling *SphereGenerate.py* and *SphereDetermine.py* as required.
- *twoTCPaths.py*: The module that handles CC paths calling *SphereGenerate.py* and *SphereDetermine.py* as required.
- *oneTCPaths.py*: The module that handles C paths calling *SphereGenerate.py* and *SphereDetermine.py* as required.

The following are miscellaneous modules in the primary set of codes:

- *Output.py*: The module handling output.
- *RigidBodyMechanics.py*: The module handling Rodrigues' rotations.

C.2 Secondary Code

The code used to construct paths of specific types and compare it with all optimal paths (by calling *IconfigFconfig.py*) is called *CCCCnonoptimality.py*.

The data sets presented in the archives consist of the data computed for corroboration of the results of Lemma 4.0.8 and hence refer to the data producing the plots figures 5.5, 5.6, 5.7, and 5.8. In addition to this, plots of the polynomial $(b_1 + b_2 + b_3)$ obtained from polynomial 4.37 for values of r considered for the other data sets are provided.

All the codes and their output files (as data sets), and relevant plots are made available in the repository as supplemental files in the zip files named "Datasets.zip" and "Codes.zip".